



MINISTRY OF SUPPLY

AERONAUTICAL RESEARCH COUNCIL
REPORTS AND MEMORANDA

Determination of the Stress Distribution in Reinforced Monocoque Structures

PART III

A Theory of Swept Wings where
the Ribs are in the Line of Flight

By

L. S. D. MORLEY

Crown Copyright Reserved

LONDON: HER MAJESTY'S STATIONERY OFFICE

1957

FIFTEEN SHILLINGS NET

Determination of the Stress Distribution in Reinforced Monocoque Structures

PART III

A Theory of Swept Wings where the Ribs are in the Line of Flight

By

L. S. D. MORLEY

COMMUNICATED BY THE PRINCIPAL DIRECTOR OF SCIENTIFIC RESEARCH (AIR),
MINISTRY OF SUPPLY

*Reports and Memoranda No. 2967**

November, 1952

Summary.—This paper gives and applies a method of estimating the stresses caused by root constraint in a two-spar swept wing of reinforced monocoque construction where the ribs are parallel to the line of flight.

The general scheme of the analysis develops the fundamental equations that govern the stresses, strains and displacements in the separate components. Then, by comparison of displacements along their inter-sections, equations of compatibility are formed. The solution of these equations yields the stress distribution and the distorted shape. In deriving the fundamental equations for the skin-stringer combination, use is made of an oblique system of co-ordinates and stresses.

A suggested numerical procedure is given for the evaluation of the stress distribution and distorted shape. It is found convenient to use matrices and the procedure has been so planned that the elements of a matrix are obtained by simple operations on the elements of preceding matrices.

A wing loading condition is also derived which produces zero rib warping, *i.e.*, there is no redistribution of stress at the root of the wing.

Tests on a cellulose-nitrate model have provided good qualitative confirmation of the theory.

1. *Introduction.*—This paper is mainly concerned with the estimation of the stresses caused by root constraint in a two-spar swept wing of reinforced monocoque construction with discrete ribs in the line of flight. The top and bottom surfaces consist of skins reinforced by numerous stringer lying parallel to the spars. Caution should be exercised in applying the method developed here to a wing with very thick skins and few or no reinforcing elements. In such a case the stresses caused by root constraint must be determined by more exact methods.

Estimation of the stress distribution in reinforced monocoque structures can be broadly considered under one of the following three headings, *viz.*,

- (a) Estimation of the overall stress distribution over regions far removed from a discontinuity (such as an abrupt change of section)
- (b) Estimation of the stress distribution in the neighbourhood of a discontinuity (*i.e.*, within a range of two or three chords)
- (c) Estimation of the peak stresses at the discontinuity (*i.e.*, within a range of two or three times the cross-sectional dimension of a relevant stiffener).

*R.A.E. Report Structures 138, received 24th February, 1953.

This paper is concerned with the stress distribution in the neighbourhood of a discontinuity (i.e., (b) above). This stress distribution is usually determined from consideration of a 'shell model' that is an appropriate and convenient idealisation of the basic reinforced monocoque structure. A theory¹ has already been developed for flat-sided structures with normal ribs, and the theory presented here for skew ribs is a special extension.

Wittrick², Hemp³ and Mansfield⁴ have produced theories for the behaviour of swept wings with ribs in the line of flight over regions far removed from a discontinuity (i.e., (a) above). They have shown that skewness of the ribs produces a coupling between the curvature and twisting of the wing box when it is under bending or torsion; and that the ribs contribute to the flexural and torsional stiffnesses. These effects are usually small and no allowance is made for them in the present theory.

2. *Description of Structure.*—2.1. *Basic Reinforced Monocoque Structure.*—The top and bottom surfaces of the two-spar wing of rectangular cross-section, shown in Fig. 1, are constructed from thin flat skins reinforced by closely spaced stringers lying parallel to the spars. The ribs are discrete and in the line of flight. Both ribs and spars are assumed unable to resist warping out of their planes.

2.2. *Derivation of the Shell Model.*—In the calculation of the stress distribution in the neighbourhood of a discontinuity account is taken only of the most important function of the individual structural components. The resulting structure with its limited attributes is called a 'shell model.'

If the cross-sectional area of the stringers is large in relation to that of the skin then the direct load parallel to the stringers is carried almost exclusively by the stringers and a condition of almost pure shear exists in the individual skin panels between any two stringers. Since the stringers are closely spaced a good approximation may be obtained by considering them as uniformly distributed over the surface of the skin. A change of shear along the skin-stringer combination can only take place at a rib. As in the analysis of unswept wing structures, the rib and spar webs are assumed to carry shear only and the booms direct load only.

The above is now applied to the case where the cross-sections of the skin and stiffeners are of the same order of value. Account is taken of the contributory direct stiffnesses of the skin by corresponding increases in the stiffener cross-sections, which are then usually called 'effective cross-sections.'

2.3. *Assumptions.*—The following assumptions are made in the analysis, *viz.*,

- (a) The stress-strain relationships are linear
- (b) Buckling is excluded
- (c) The stringers and booms can resist only direct load
- (d) The stringers are so closely spaced that they may be considered uniformly distributed over the surface of the skin
- (e) The skin and spar webs can resist only shear, account being taken of their contributory direct stiffnesses by corresponding increases in the stiffener and boom cross-sections. In particular for the skin, a condition of pure shear exists between any two stringers in the direction of the stringers, irrespective of rib direction
- (f) The ribs cannot resist warping out of their plane and the rib webs can only resist shear.

A further assumption that the rib booms are inextensional is made to simplify the computation.

3. *Determination of the Stress Distribution.*—3.1. *Analysis.*—Full details of the analysis for the above shell model are given in Appendix I. The first step in the analysis is to form the differential equations of compatibility for the top and bottom skin-stringer combinations, and for these it has been found convenient to use the oblique system of co-ordinates as described by Hemp³. When the rib booms are considered inextensional the equations of compatibility

reduce to a set of n simultaneous differential equations of the second order, where n is the number of bays in the shell model. An explicit solution of these equations can be found when the rib spacings are assumed constant; and it is shown in Appendix VII that this solution is

$$\bar{T}_j = \bar{T}_n + \sum_{k=1}^n C_k \exp \{ \lambda_k(\mathbf{y}/L) \} \cdot \left(\frac{\lambda_k^2 + A\lambda_k + B}{\lambda_k^2 - A\lambda_k + B} \right)^{j/2} \cos \frac{\pi(2k-1)j}{2n}$$

$$+ \sum_{k=1}^n c_k \exp \{ -\lambda_k(\mathbf{y}/L) \} \cdot \left(\frac{\lambda_k^2 + A\lambda_k + B}{\lambda_k^2 - A\lambda_k + B} \right)^{-j/2}$$

where $\bar{T}_j = T_j(\mathbf{x} = L) \sin \alpha - 2S_j \cos \alpha$
 $= T_{j+1}(\mathbf{x} = 0) \sin \alpha - 2S_{j+1} \cos \alpha$ } and is called the oblique-stress resultant in the skin-stringer combination at the j th rib,

T_j is the direct-stress resultant along a stringer in the j th bay of the skin-stringer combination,

S_j shear-stress resultant in the j th bay of the skin-stringer combination,

\mathbf{x} distance along a stringer, a new origin being chosen on the left-hand side of each bay,

L distance between ribs measured along a stringer,

$A = 12 \cos \alpha$,

$B = 6 \left(\frac{Et^*}{\mu t} \sin^2 \alpha + 4 \cos^2 \alpha \right)$,

$C_k, c_k =$ arbitrary constants.

The λ_k are the roots of the quadratics

$$(2\lambda_k^2 - B)^2 \sin^2 \frac{\pi(2k-1)}{2n} - \lambda_k^2 (6B - A^2 - 3\lambda_k^2) \cos^2 \frac{\pi(2k-1)}{2n} = 0$$

and depend only on the non-dimensional structural parameters A and B , the current suffix k and the number of bays.

The shear-stress resultants S_j are then found to be

$$S_j = -\frac{A}{B} \bar{T}_n + \frac{6Et^* \sin \alpha}{BL} (\bar{V}_j - \bar{V}_{j-1})$$

$$+ \sum_{k=1}^n \frac{1}{\lambda_k} \left[\begin{aligned} & C_k \exp \{ \lambda_k(\mathbf{y}/L) \} \cdot \left\{ \left(\frac{\lambda_k^2 + A\lambda_k + B}{\lambda_k^2 - A\lambda_k + B} \right)^{j/2} \cos \frac{\pi(2k-1)j}{2n} \right. \\ & \left. - \left(\frac{\lambda_k^2 + A\lambda_k + B}{\lambda_k^2 - A\lambda_k + B} \right)^{(j-1)/2} \cos \frac{\pi(2k-1)(j-1)}{2n} \right\} \\ & - c_k \exp \{ -\lambda_k(\mathbf{y}/L) \} \cdot \left\{ \left(\frac{\lambda_k^2 + A\lambda_k + B}{\lambda_k^2 - A\lambda_k + B} \right)^{-j/2} \cos \frac{\pi(2k-1)j}{2n} \right. \\ & \left. - \left(\frac{\lambda_k^2 + A\lambda_k + B}{\lambda_k^2 - A\lambda_k + B} \right)^{-(j-1)/2} \cos \frac{\pi(2k-1)(j-1)}{2n} \right\} \end{aligned} \right]$$

where the \bar{V}_j refer to rib displacements.

It should be noted that the 'oblique-stress resultants' \mathbf{T} are continuous at a rib because the ribs cannot resist warping out of their plane. Now, the true direct-stress resultant T along a stringer is determined from the relationship

$$T = \mathbf{T} \operatorname{cosec} \alpha + 2S \cot \alpha$$

and is, in general, discontinuous at a rib.

It remains to determine the value of the arbitrary constants C_k, c_k and also the \bar{V}_j . These are found from considerations of equilibrium and comparing displacements of the component parts of the shell model. In general, this procedure results in a set of $3n$ simultaneous equations. It is shown in Appendix VIII that the whole procedure is consistent with the total strain energy stored in the shell model being rendered a minimum.

In Appendix II it is shown that when the shell model contains simultaneously elementary bending and torsion distributions such that

$$\frac{\mathbf{T}'}{S'} = -\frac{Et^* \tan \alpha}{\mu t} \left\{ \sin \alpha - \frac{1}{2} \left(\frac{b}{a} \right) \left(\frac{t}{t_R} + \frac{t}{t_F} \right) \right\},$$

where \mathbf{T}' and S' are constants referring respectively to the bending and torsion, there is then no warping of the ribs. The resultant of these stress distributions corresponds to a vector couple inclined at an angle ψ from the stringers (Fig. 1) where

$$\tan \psi = -\frac{\mathbf{T}' \operatorname{cosec} \alpha}{S'} \left\{ 1 + \frac{\operatorname{cosec} \alpha}{2at^*} (A_R + A_F) \right\}$$

and where \mathbf{T}'/S' is as given above. The vanishing of the rib warping means of course that there is no redistribution of stress when the wing structure is built in at a rib. There will, however, be a redistribution of stress in the vicinity of the applied couple unless it is applied in a manner corresponding to the elementary distributions.

3.2. Numerical Application.—Full details of the numerical procedure for the evaluation of the stress distribution and deflections are given in Appendix IV, and a numerical illustrative example is given in Appendix V.

It can be seen on reference to the foregoing equations that the numerical work involved in their evaluation will be considerable. An analysis of the unswept wing usually requires the solution of the 'shear lag' problem⁵ presented when the wing is resisting a normal force loading, and also requires the *separate* solution of an 'end constraint'⁶ problem arising when the wing is under torsion. The analysis of the swept wing does not, however, appear to permit a comparable separation of problems. This, coupled with the loss of orthogonal relations between the functions, means that the numerical work will inevitably be considerable in the corresponding calculations for a swept wing.

In applying the analysis to a particular structure it is preferable to keep the numerical work down to a minimum, and this can only be achieved by restricting the number of bays to be investigated. Thus the problem arises whether to replace a given wing structure by

- (a) a shell model of the same overall dimensions with an increased distance between the equally spaced ribs
- (b) a shorter shell model in which the correct distance is retained between the equally spaced ribs
- (c) a shell model in which the rib spacings are unequal.

In this paper the first choice has been adopted and good experimental agreement was obtained. (The experimental results were obtained from the cellulose-nitrate model described in Appendix VI and should be regarded as qualitative verification of the theoretical results.) It is possible, nevertheless, for wings of other configurations that a rib nearer the root will appreciably influence the stress distribution.

LIST OF SYMBOLS—*continued*

Co-ordinate system

j	Current bay or rib number
k	Integer such that $0 < k \leq n$
n	Total number of bays in the shell model
x	Rectangular co-ordinate along a stringer ; a new origin being chosen on the left-hand side of each bay
x	Oblique co-ordinate along a stringer, a new origin being chosen on the left-hand side of each bay
y	Rectangular co-ordinate normal to a stringer but in the plane of the skin-stringer combination ; origin at the centre stringer
y	Oblique co-ordinate parallel to the ribs and in the plane of the skin-stringer combination ; origin at the centre stringer
z	Normal co-ordinate with origin midway between top and bottom skin-stringer combinations

Loads and stresses

M_j	Couple applied to and in the plane of the j th rib
P_{Fj}	End load in the front spar in the j th bay
P_{Rj}	End load in the rear spar in the j th bay
\bar{P}_{Fj}	End load in the front spar at the j th rib
\bar{P}_{Rj}	End load in the rear spar at the j th rib
S_j	Shear-stress resultant in the j th bay of the skin-stringer combination
$S_j(a)$	Value of the shear-stress resultant at $y = a$, i.e., at the rear spar
$S_j(-a)$	Value of the shear-stress resultant at $y = -a$, i.e., at the front spar
S_{Fj}	Shear-stress resultant in the j th bay of the front spar web
S_{Rj}	Shear-stress resultant in the j th bay of the rear spar web
S'	Particular value of the shear-stress resultant
\bar{S}_j	Shear-stress resultant in the j th rib
T_j	Direct-stress resultant along a stringer in the j th bay of the skin-stringer combination
\mathbf{T}_j	Oblique-stress resultant in the j th bay of the skin-stringer combination
\mathbf{T}'	Particular value of the oblique-stress resultant
$\bar{\mathbf{T}}_j$	Oblique-stress resultant in the skin-stringer combination at the j th rib
W_j	z -wise load applied to the j th rib

Strains and displacements

e_{xx}	Direct strain along a stringer
e_{xy}	Shear strain in the skin-stringer combination
e_{yy}	Direct strain normal to a stringer but in the plane of the skin-stringer combination

LIST OF SYMBOLS—*continued*

e_{xx}	Oblique-strain component along a stringer	}	defined in equation (6)
e_{xy}	Oblique-strain component in the skin-stringer combination		
e_{yy}	Oblique-strain component parallel to the ribs and in the plane of the skin-stringer combination		
U_j	Displacement along a stringer in the j th bay		
$U_j(a)$	Value of the displacement at $y = a$, i.e., at the rear spar		
$U_j(-a)$	Value of the displacement at $y = -a$, i.e., at the front spar		
u_{Fj}	Displacement along the front spar in the j th bay		
U_{Fj}	Displacement along the front spar boom in the j th bay		
u_{Rj}	Displacement along the rear spar in the j th bay		
U_{Rj}	Displacement along the rear spar boom in the j th bay		
\bar{U}_j	Displacement along a stringer at the j th rib		
\bar{U}_{Fj}	Displacement along the front spar boom at the j th rib		
\bar{U}_{Rj}	Displacement along the rear spar boom at the j th rib		
V_j	Oblique-displacement component in the j th bay, it is parallel to the ribs and in the plane of the skin-stringer combination		
\bar{v}_j	Displacement parallel to the rib booms in the j th rib		
\bar{V}_j	Oblique-displacement component in the skin-stringer combination at the j th rib, this being identical to the displacement of the rib boom		
w_{Fj}	z -wise displacement of the front spar web in the j th bay		
w_{Rj}	z -wise displacement of the rear spar web in the j th bay		
\bar{w}_j	z -wise displacement of the j th rib web		
\bar{w}_{Fj}	z -wise displacement of the front spar web at the j th rib		
\bar{w}_{Rj}	z -wise displacement of the rear spar web at the j th rib		
\bar{w}_{0j}	z -wise displacement at the centre of the j th rib web		

Elastic constants

E	Young's modulus of elasticity for the structure
μ	Shear modulus for the structure

Additional symbols are used in Appendices IV to VIII but these are defined as they are introduced.

REFERENCES

No.	Author	<i>Title, etc.</i>
1	L. S. D. Morley	Determination of the stress distribution in reinforced monocoque structures. Part I. A theory of flat sided structures. R. & M. 2879. December, 1951.
2	W. H. Wittrick	Preliminary analysis of a highly swept cylindrical tube under torsion and bending. Aeronautical Research Report ACA-39. May, 1948.
3	W. S. Hemp	On the application of oblique co-ordinates to problems of plane elasticity and swept wings. College of Aeronautics Report 31. R. & M. 2754. January, 1950.
4	E. H. Mansfield	Elasticity of a sheet reinforced by stringers and skew ribs, with applications to swept wings. R. & M. 2758. December, 1949.
5	D. Williams, R. D. Starkey and A. H. Taylor	Distribution of stress between spar flanges and stringers for a wing under distributed loading. R. & M. 2098. June, 1939.
6	H. L. Cox	On the stressing of polygonal tubes with particular reference to the torsion of tapered tubes of trapezoidal section. R. & M. 1908. December, 1942.
7	D. Williams	Torsion of a rectangular tube with axial constraints. R. & M. 1619. May, 1934.
8	L. S. D. Morley and N. S. Heaps ..	Experiments to determine the effect of root constraint in a swept wing. R.A.E. Tech. Note Structures 108. A.R.C. 16,064. March, 1953.

APPENDIX I

Determination of the Stress Distribution

In preparation for forming the equations of compatibility for the wing structure shown in Fig. 1 it is necessary to consider the detailed equations governing the individual behaviours of the skin-stringer combination, ribs and spars. It is demonstrated in Appendix VIII that these equations are consistent with the strain energy stored in the structure being rendered a minimum.

1. *Oblique Co-ordinates and Stress Systems for the Skin-Stringer Combination.*—It is most convenient to use the oblique system of co-ordinates shown in Fig. 2. The rectangular system is denoted by italic characters and the oblique system by bold italic characters.

A transformation from the rectangular to the oblique system is effected by

$$\left. \begin{aligned} x &= \mathbf{x} + \mathbf{y} \cos \alpha \\ y &= \mathbf{y} \sin \alpha \end{aligned} \right\} \dots \dots \dots (1)$$

Similarly, the respective transformations for the displacements are

$$\left. \begin{aligned} u &= \mathbf{u} + \mathbf{v} \cos \alpha \\ v &= \mathbf{v} \sin \alpha \end{aligned} \right\} \dots \dots \dots (2)$$

It is to be noted that the projected displacements in the \mathbf{x} - and \mathbf{y} -wise directions are respectively

$$\left. \begin{aligned} \mathbf{U} &= u = \mathbf{u} + \mathbf{v} \cos \alpha \\ \mathbf{V} &= \mathbf{u} \cos \alpha + \mathbf{v} \end{aligned} \right\} \dots \dots \dots (3)$$

The oblique and rectangular systems of stress resultants are shown in Fig. 3. The transformation from the rectangular to the oblique system is

$$\left. \begin{aligned} T &= \mathbf{T} \operatorname{cosec} \alpha + 2\mathbf{S} \cot \alpha \\ S &= \mathbf{s} \end{aligned} \right\} \dots \dots \dots (4)$$

2. *Fundamental Equations for the Skin-Stringer Combination.*—In what follows attention is confined to cases where the displacements at $z = \pm b$ are equal and opposite to one another.

It is now proposed to develop the fundamental equations for the top surface skin-stringer combination using the oblique co-ordinates and stress systems just derived.

The oblique system of stress resultants acting on an elemental portion of skin-stringer combination are shown in Fig. 4. For equilibrium it is necessary that

$$\frac{\partial \mathbf{T}_j}{\partial \mathbf{x}} + \frac{\partial S_j}{\partial \mathbf{y}} = 0 \quad \dots \dots \dots \quad (5)$$

In deriving the stress, strain and displacement relationships, it is convenient to introduce a set of oblique strain components by the strain quadric

$$e_{xx}x^2 + e_{xy}xy + e_{yy}y^2 = \mathbf{e}_{xx}\mathbf{x}^2 + \mathbf{e}_{xy}\mathbf{x}\mathbf{y} + \mathbf{e}_{yy}\mathbf{y}^2.$$

On substitution from equation (1) it is seen that

$$\left. \begin{aligned} \mathbf{e}_{xx} &= e_{xx} \\ \mathbf{e}_{xy} &= 2e_{xx} \cos \alpha + e_{xy} \sin \alpha \\ \mathbf{e}_{yy} &= e_{xx} \cos^2 \alpha + e_{xy} \sin \alpha \cos \alpha + e_{yy} \sin^2 \alpha \end{aligned} \right\}, \quad \dots \dots \dots \quad (6)$$

and it can be shown on using equations (1) to (3) that these oblique strain components may be determined from

$$\left. \begin{aligned} \mathbf{e}_{xx} &= \frac{\partial \mathbf{U}}{\partial \mathbf{x}} \\ \mathbf{e}_{xy} &= \frac{\partial \mathbf{U}}{\partial \mathbf{y}} + \frac{\partial \mathbf{V}}{\partial \mathbf{x}} \\ \mathbf{e}_{yy} &= \frac{\partial \mathbf{V}}{\partial \mathbf{y}} \end{aligned} \right\} \dots \dots \dots \quad (7)$$

It is, of course, recognised from the last of equations (6) that \mathbf{e}_{yy} is the true strain component in the \mathbf{y} -wise direction. The strains in terms of the stress resultants and referred to the rectangular system of axes are

$$\left. \begin{aligned} e_{xx} &= \frac{\partial u}{\partial x} = \frac{T}{Et^*} \\ e_{xy} &= \frac{\partial u}{\partial y} + \frac{\partial v}{\partial x} = \frac{S}{\mu t} \end{aligned} \right\} \dots \dots \dots \quad (8)$$

Now, a change of shear along the skin-stringer combination can only take place at a rib (i.e., S is independent of \mathbf{x}) and equation (5) may be integrated to give

$$\mathbf{T}_j = -\mathbf{x} \frac{dS_j}{d\mathbf{y}} + \bar{\mathbf{T}}_{j-1} \quad \dots \dots \dots \quad (9)$$

where a new origin for \mathbf{x} is chosen on the left-hand side of each bay and $\bar{\mathbf{T}}_{j-1}$ denotes the value of the oblique stress resultant in the skin-stringer combination at the $(j-1)$ th rib. It follows that \mathbf{T} must be continuous along a stringer because a rib cannot resist warping out of its plane.

From equations (4), (6), (7) and (8) it is seen that

$$\frac{\partial \mathbf{U}_j}{\partial \mathbf{x}} = \frac{1}{Et^*} (\mathbf{T}_j \operatorname{cosec} \alpha + 2S_j \cot \alpha)$$

so, on substituting from equation (9) and integrating, it is found that

$$\mathbf{U}_j = \frac{1}{Et^*} \left(-\frac{\mathbf{x}^2}{2} \frac{dS_j}{dy} \operatorname{cosec} \alpha + \mathbf{x} \bar{\mathbf{T}}_{j-1} \operatorname{cosec} \alpha + 2\mathbf{x} S_j \cot \alpha \right) + \bar{\mathbf{U}}_{j-1} \quad \dots \quad (10)$$

where $\bar{\mathbf{U}}_{j-1}$ is the displacement component at the $(j-1)$ th rib. Again from equations (4), (6), (7) and (8)

$$\frac{\partial \mathbf{U}_j}{\partial \mathbf{y}} + \frac{\partial \mathbf{V}_j}{\partial \mathbf{x}} = \frac{1}{\mu t} S_j \sin \alpha + \frac{1}{Et^*} \{ 2\bar{\mathbf{T}}_j \cot \alpha + 4S_j \cot \alpha \cos \alpha \}$$

which, on substitution from equations (9) and (10) and integrating, yields

$$\begin{aligned} \mathbf{V}_j = & \frac{\mathbf{x}}{\mu t} S_j \sin \alpha - \frac{1}{Et^*} \left\{ -\frac{\mathbf{x}^3}{6} \frac{d^2 S_j}{dy^2} \operatorname{cosec} \alpha + \frac{\mathbf{x}^2}{2} \frac{d\bar{\mathbf{T}}_{j-1}}{dy} \operatorname{cosec} \alpha \right. \\ & + 2\mathbf{x}^2 \frac{dS_j}{dy} \cot \alpha - 2\mathbf{x} \bar{\mathbf{T}}_{j-1} \cot \alpha - 4\mathbf{x} S_j \cos \alpha \cot \alpha \left. \right\} \\ & - \mathbf{x} \frac{d\bar{\mathbf{U}}_{j-1}}{dy} + \bar{\mathbf{V}}_{j-1}, \quad \dots \quad \dots \quad \dots \quad \dots \quad \dots \quad \dots \quad \dots \quad \dots \quad \dots \quad \dots \quad (11) \end{aligned}$$

where $\bar{\mathbf{V}}_{j-1}$ denotes the displacement component at the $(j-1)$ th rib.

Putting $\mathbf{x} = L$ in this equation yields

$$\begin{aligned} & \frac{L}{\mu t} S_j \sin \alpha - \frac{1}{Et^*} \left\{ -\frac{L^3}{6} \frac{d^2 S_j}{dy^2} \operatorname{cosec} \alpha + \frac{L^2}{2} \frac{d\bar{\mathbf{T}}_{j-1}}{dy} \operatorname{cosec} \alpha + 2L^2 \frac{dS_j}{dy} \cot \alpha \right. \\ & \left. - 2L \bar{\mathbf{T}}_{j-1} \cot \alpha - 4L S_j \cos \alpha \cot \alpha \right\} - L \frac{d\bar{\mathbf{U}}_{j-1}}{dy} \\ & = \bar{\mathbf{V}}_j - \bar{\mathbf{V}}_{j-1}. \quad \dots \quad \dots \quad \dots \quad \dots \quad \dots \quad \dots \quad \dots \quad \dots \quad \dots \quad \dots \quad (12) \end{aligned}$$

Manipulation of equations (9) to (12) yields

$$\begin{aligned} & \left(L^2 \frac{d^2}{dy^2} + AL \frac{d}{dy} + B \right) \bar{\mathbf{T}}_{j-1} + 2 \left(2L^2 \frac{d^2}{dy^2} - B \right) \bar{\mathbf{T}}_j + \left(L^2 \frac{d^2}{dy^2} - AL \frac{d}{dy} + B \right) \bar{\mathbf{T}}_{j+1} \\ & = -6Et^* \sin \alpha \frac{d}{dy} (\bar{\mathbf{V}}_{j-1} - 2\bar{\mathbf{V}}_j + \bar{\mathbf{V}}_{j+1}) \quad \dots \quad \dots \quad \dots \quad \dots \quad \dots \quad (13) \end{aligned}$$

where A and B are non-dimensional structural parameters defined as

$$A = 12 \cos \alpha,$$

$$B = 6 \left(\frac{Et^*}{\mu t} \sin^2 \alpha + 4 \cos^2 \alpha \right).$$

At the wing root $\bar{\mathbf{U}}_0$ and $\bar{\mathbf{V}}_0$ are zero and the equation appropriate to (13) is then

$$\left(2L^2 \frac{d^2}{dy^2} - B \right) \bar{\mathbf{T}}_0 + \left(L^2 \frac{d^2}{dy^2} - AL \frac{d}{dy} + B \right) \bar{\mathbf{T}}_1 = -6Et^* \sin \alpha \frac{d\bar{\mathbf{V}}_1}{dy} \quad \dots \quad (14)$$

Finally, at the free end of the wing the direct-stress resultants $\bar{\mathbf{T}}_n$ will be specified and equation (13) becomes

$$\begin{aligned} & \left(L^2 \frac{d^2}{dy^2} + AL \frac{d}{dy} + B \right) \bar{\mathbf{T}}_{n-2} + 2 \left(2L^2 \frac{d^2}{dy^2} - B \right) \bar{\mathbf{T}}_{n-1} \\ & = - \left(L^2 \frac{d^2}{dy^2} - AL \frac{d}{dy} + B \right) \bar{\mathbf{T}}_n - 6Et^* \sin \alpha \frac{d}{dy} (\bar{\mathbf{V}}_{n-2} - 2\bar{\mathbf{V}}_{n-1} + \bar{\mathbf{V}}_n) \quad \dots \quad (15) \end{aligned}$$

If the rib booms are considered inextensional the $d\bar{\mathbf{v}}/d\mathbf{y}$ are all zero and it is shown in Appendix VII that the solution to the above fundamental equations (13), (14) and (15) is then

$$C_k \exp \{ \lambda_k(\mathbf{y}/L) \} \cdot \left(\frac{\lambda_k^2 + A\lambda_k + B}{\lambda_k^2 - A\lambda_k + B} \right)^{j/2} \cos \frac{\pi(2k-1)j}{2n}, \quad (16)$$

$$\bar{\mathbf{T}}_j = \bar{\mathbf{T}}_n + \sum_{k=1}^n$$

$$c_k \exp \{ -\lambda_k(\mathbf{y}/L) \} \cdot \left(\frac{\lambda_k^2 + A\lambda_k + B}{\lambda_k^2 - A\lambda_k + B} \right)^{-j/2}$$

where C_k and c_k are arbitrary constants and where $\bar{\mathbf{T}}_n$ has been assumed constant. The roots λ_k are determined from the quadratics

$$(2\lambda_k^2 - B)^2 \sin^2 \frac{\pi(2k-1)}{2n} - \lambda_k^2 (6B - A^2 - 3\lambda_k^2) \cos^2 \frac{\pi(2k-1)}{2n} = 0 \quad \dots \quad (17)$$

where $\lambda_k < \lambda_{n-k+1}$.

From equation (9) it is seen that

$$L \frac{dS_j}{d\mathbf{y}} = -(\bar{\mathbf{T}}_j - \bar{\mathbf{T}}_{j-1})$$

which, on substitution from equation (16) and integrating, yields

$$S_j = -\frac{A}{B} \bar{\mathbf{T}}_n + \frac{6Et^* \sin \alpha}{BL} (\bar{\mathbf{v}}_j - \bar{\mathbf{v}}_{j-1})$$

$$\left[\begin{array}{l} C_k \exp \{ \lambda_k(\mathbf{y}/L) \} \cdot \left\{ \left(\frac{\lambda_k^2 + A\lambda_k + B}{\lambda_k^2 - A\lambda_k + B} \right)^{j/2} \cos \frac{\pi(2k-1)j}{2n} \right. \\ \left. - \left(\frac{\lambda_k^2 + A\lambda_k + B}{\lambda_k^2 - A\lambda_k + B} \right)^{(j-1)/2} \cos \frac{\pi(2k-1)(j-1)}{2n} \right\} \\ - \sum_{k=1}^n \frac{1}{\lambda_k} \left[\begin{array}{l} -c_k \exp \{ -\lambda_k(\mathbf{y}/L) \} \cdot \left\{ \left(\frac{\lambda_k^2 + A\lambda_k + B}{\lambda_k^2 - A\lambda_k + B} \right)^{-j/2} \cos \frac{\pi(2k-1)j}{2n} \right. \\ \left. - \left(\frac{\lambda_k^2 + A\lambda_k + B}{\lambda_k^2 - A\lambda_k + B} \right)^{-(j-1)/2} \cos \frac{\pi(2k-1)(j-1)}{2n} \right\} \end{array} \right] \end{array} \right] \quad (18)$$

where the constants of integration have been determined from equation (12).

3. *Fundamental Equations for the Spar Booms.*—The spar booms are additional end load carrying members attached along the outer edges of the skin-stringer combination. They are massive in comparison with the adjacent stringer. The forces acting on an elemental portion of the rear spar boom are shown in Fig. 5. For equilibrium of this element it is necessary that

$$\frac{dP_{Rj}}{d\mathbf{x}} = S_{Rj} + S_j(a) .$$

On integration, this yields

$$P_{Rj} = \mathbf{x} \{ S_{Rj} + S_j(a) \} + \bar{P}_{Rj-1} \quad \dots \quad \dots \quad \dots \quad \dots \quad \dots \quad (19)$$

where \bar{P}_{Rj-1} denotes the end load in the rear spar boom at the $(j - 1)$ th rib. Proceeding in a similar manner for the front spar boom it is found that

$$P_{Fj} = \mathbf{x}\{S_{Fj} - S_j(-a)\} + \bar{P}_{Fj-1} \dots \dots \dots \dots \dots \dots \dots \dots \dots \dots \quad (20)$$

Now, the end load in a spar boom is continuous at a rib whereas the direct-stress resultant T (orthogonal system) in the skin-stringer combination is, in general, discontinuous at a rib. There is then a discontinuity of displacement between a spar boom and the adjacent stringer. It is therefore necessary to relax the usual condition of continuity of displacement to an average requirement such that

$$\int_0^L \mathbf{U}_{Rj} d\mathbf{x} = \int_0^L \mathbf{U}_j(a) d\mathbf{x} \dots \dots \dots \dots \dots \dots \dots \dots \dots \dots \quad (21)$$

where \mathbf{U}_{Rj} denotes the displacement along the rear spar boom in the j th bay and $\mathbf{U}_j(a)$ denotes the corresponding displacement along the adjacent stringer. From equation (19), it is readily seen that

$$\mathbf{U}_{Rj} = \frac{1}{EA_R} \left[\frac{x^2}{2} \{S_{Rj} + S_j(a)\} + \mathbf{x}\bar{P}_{Rj-1} \right] + \bar{\mathbf{U}}_{Rj-1} \dots \dots \dots \dots \quad (22)$$

where A_R is the effective cross-sectional area of the rear spar boom (*i.e.*, the nominal boom area plus effective skin and spar web area) and $\bar{\mathbf{U}}_{Rj-1}$ denotes the displacement at the $(j - 1)$ th rib. Integrating equation (22) yields

$$\int_0^L \mathbf{U}_{Rj} d\mathbf{x} = \frac{1}{EA_R} \left[\frac{L^3}{6} \{S_{Rj} + S_j(a)\} + \frac{L^2}{2} \bar{P}_{Rj-1} \right] + L\bar{\mathbf{U}}_{Rj-1} \dots \dots \dots \quad (23)$$

and integrating equation (10) yields

$$\int_0^L \mathbf{U}_j(a) d\mathbf{x} = \left[\frac{1}{Et^*} \left\{ -\frac{L^3}{6} \frac{dS_j}{dy} \operatorname{cosec} \alpha + \frac{L^2}{2} \bar{T}_{j-1} \operatorname{cosec} \alpha + L^2 S_j \cot \alpha \right\} + L\bar{\mathbf{U}}_{j-1} \right]_{y=a} \quad (24)$$

Substitution of equations (23) and (24) into (21) then yields the compatibility equation between the rear spar boom and adjacent stringer.

Similarly, for the front spar boom it is necessary that

$$\int_0^L \mathbf{U}_{Fj} d\mathbf{x} = \int_0^L \mathbf{U}_j(-a) d\mathbf{x} \dots \dots \dots \dots \dots \dots \dots \dots \dots \dots \quad (25)$$

where \mathbf{U}_{Fj} denotes the displacement along the front spar boom in the j th bay and $\mathbf{U}_j(-a)$ denotes the corresponding displacement along the adjacent stringer. From equation (20), the boom displacement is

$$\mathbf{U}_{Fj} = \frac{1}{EA_F} \left[\frac{x^2}{2} \{S_{Fj} - S_j(-a)\} + \mathbf{x}\bar{P}_{Fj-1} \right] + \bar{\mathbf{U}}_{Fj-1} \dots \dots \dots \dots \quad (26)$$

On integration this becomes

$$\int_0^L \mathbf{U}_{Fj} d\mathbf{x} = \frac{1}{EA_F} \left[\frac{L^3}{6} \{S_{Fj} - S_j(-a)\} + \frac{L^2}{2} \bar{P}_{Fj-1} \right] + L\bar{\mathbf{U}}_{Fj-1} \dots \dots \dots \quad (27)$$

and integrating equation (10) yields

$$\int_0^L \mathbf{U}_j(-a) d\mathbf{x} = \left[\frac{1}{Et^*} \left\{ -\frac{L^3}{6} \frac{dS_j}{dy} \operatorname{cosec} \alpha + \frac{L^2}{2} \bar{\mathbf{T}}_{j-1} \operatorname{cosec} \alpha + L^2 S_j \cot \alpha \right\} + L \bar{\mathbf{U}}_{j-1} \right]_{y=-a} \dots \dots \dots \dots \dots \dots (28)$$

Substitution of equations (27) and (28) into (25) then yields the compatibility equation between the front spar boom and adjacent stringer.

4. *Fundamental Equations for the Ribs and Spar Webs.*—The co-ordinate system for and forces acting on the j th rib are shown in Fig. 6. Since the rib flanges are considered inextensional the shear flow acting on the rib is constant and is denoted by \bar{S}_j .

For a pure shear carrying rib the strain equation is

$$\frac{\partial \bar{w}_j}{\partial y} + \frac{\partial \bar{v}_j}{\partial z} = \frac{\bar{S}_j}{\mu \bar{t}}$$

The displacement condition for such a rib is not well defined so, for simplicity, it will be assumed that \bar{w}_j is independent of z . Differentiation of the strain equation with respect to z then shows that

$$\bar{v}_j = \frac{z}{b} \bar{\mathbf{V}}_j,$$

since at $z = \pm b$ the rib displacements must conform with those of the skin-stringer combination. This, and the strain equation then yield

$$\bar{w}_j = \frac{y \bar{S}_j}{\mu \bar{t}} - \frac{y}{b} \bar{\mathbf{V}}_j + \bar{w}_{0j} \dots \dots \dots \dots \dots \dots (29)$$

where \bar{w}_{0j} is the vertical displacement of the rib at $y = 0$.

The co-ordinate systems for and the forces acting on the front and rear spar webs in the j th bay are shown in Fig. 7. Agreement of the z -wise displacements w_{Fj} and w_{Rj} with the displacement \bar{w}_j of the rib show that the former are also independent of the z co-ordinate. For the rear spar web, the strain equation is

$$\frac{\partial w_{Rj}}{\partial \mathbf{x}} + \frac{\partial u_{Rj}}{\partial z} = \frac{S_{Rj}}{\mu t_R}$$

Differentiation of this equation with respect to z then shows that

$$u_{Rj} = \frac{z}{b} \mathbf{U}_{Rj}$$

since at $z = \pm b$ the spar web displacements must agree with those of the spar boom. This, and the strain equation then yield

$$w_{Rj} = \frac{\mathbf{x} S_{Rj}}{\mu t_R} - \frac{1}{b} \int_0^{\mathbf{x}} \mathbf{U}_{Rj} d\mathbf{x} + \bar{w}_{Rj-1} \dots \dots \dots \dots \dots \dots (30)$$

where \bar{w}_{Rj-1} is the z -wise displacement of the spar web at the $(j-1)$ th rib. Similarly, for the front spar web,

$$w_{Fj} = \frac{\mathbf{x} S_{Fj}}{\mu t_F} - \frac{1}{b} \int_0^{\mathbf{x}} \mathbf{U}_{Fj} d\mathbf{x} + \bar{w}_{Fj-1} \dots \dots \dots \dots \dots \dots (31)$$

Noting that

$$\begin{aligned}\bar{w}_j(\mathbf{y} = a) &= \bar{w}_{Rj} \\ \bar{w}_j(\mathbf{y} = -a) &= \bar{w}_{Fj}\end{aligned}$$

it is easily shown that

$$\bar{w}_{0j} - \bar{w}_{0j-1} = \frac{LS_{Rj}}{2\mu t_R} + \frac{LS_{Fj}}{2\mu t_F} - \frac{1}{2b} \int_0^L (\mathbf{U}_{Rj} + \mathbf{U}_{Fj}) d\mathbf{x}, \quad \dots \dots \dots \quad (32)$$

and

$$\begin{aligned}\bar{\mathbf{v}}_j - \bar{\mathbf{v}}_{j-1} &= -\frac{Lb}{2a\mu t_R} S_{Rj} + \frac{Lb}{2a\mu t_F} S_{Fj} \\ &+ \frac{1}{2a} \int_0^L (\mathbf{U}_{Rj} - \mathbf{U}_{Fj}) d\mathbf{x} + \frac{b}{\mu t} (\bar{S}_j - \bar{S}_{j-1}) \dots \dots \dots \quad (33)\end{aligned}$$

5. *Equations of Overall Equilibrium.*—To complete the formulation it now remains only to determine the equations of overall equilibrium for the structure under the system of loading shown in Fig. 8.

The equations of overall equilibrium are obtained most easily by consideration of the equilibrium of the j th rib. Resolving forces in the z -wise direction it is necessary that

$$S_{Rj} + S_{Fj} = -\frac{1}{2b} \sum_{i=j}^n W_i \dots \dots \dots \quad (34)$$

Resolving moments in the plane of the rib, it is found that

$$S_{Rj} - S_{Fj} - \frac{1}{a} \int_{-a}^a S_j dy = -\frac{1}{2ab} \sum_{i=j}^n M_i \dots \dots \dots \quad (35)$$

These last two equations are independent of the manner of application of the loads W and M . It will be assumed that the loads are applied such that the shear \bar{S}_j in the j th rib is given by

$$\bar{S}_j = \frac{1}{2a} \int_{-a}^a (S_{j+1} - S_j) d\mathbf{y} + \frac{M_j}{8ab} \dots \dots \dots \quad (36)$$

The stress distribution in the immediate vicinity of the applied load will, of course, depend upon the precise mode of application.

APPENDIX II

Condition for Zero Warping of the Ribs in the Shell Model

Far from a discontinuity it is to be expected that the stresses in the shell model will settle down to those given by the elementary theories and be independent of the rib direction. It is of particular interest to examine the behaviour of the shell model when it contains only the elementary bending and torsion stresses.

The elementary bending distribution is defined by

$$\left. \begin{aligned} S_j &= 0 \\ \mathbf{T}_j &= \mathbf{T}' = \text{a constant} \\ S_{Rj} &= S_{Fj} = 0 \\ P_{Rj} &= \frac{A_R}{t^*} \mathbf{T}' \operatorname{cosec} \alpha \\ P_{Fj} &= \frac{A_F}{t^*} \mathbf{T}' \operatorname{cosec} \alpha \end{aligned} \right\} \dots \dots \dots \dots \quad (37)$$

where it is to be noted that the boom end loads are such that equality of strain exists between a boom and the adjacent stringer. From equations (10) and (12) it is seen that the displacement components in the skin-stringer combination are

$$\begin{aligned} \bar{\mathbf{U}}_j &= \frac{\mathbf{T}'L}{Et^*} \operatorname{cosec} \alpha + \bar{\mathbf{U}}_{j-1}, \\ \bar{\mathbf{V}}_j - \bar{\mathbf{V}}_{j-1} &= \frac{2\mathbf{T}'L}{Et^*} \cot \alpha - L \frac{d\bar{\mathbf{U}}_{j-1}}{dy}, \end{aligned}$$

and the boom displacements are

$$\bar{\mathbf{U}}_{Rj} = \bar{\mathbf{U}}_j(a) \quad \text{and} \quad \bar{\mathbf{U}}_{Fj} = \bar{\mathbf{U}}_j(-a).$$

From equation (33) and using equations (21), (24), (25) and (28) it follows that

$$\bar{\mathbf{V}}_j - \bar{\mathbf{V}}_{j-1} = \frac{L}{2a} \left[\bar{\mathbf{U}}_{j-1} \right]_{-a}^a$$

and therefore from above,

$$\frac{L}{2a} \left[\bar{\mathbf{U}}_{j-1} \right]_{-a}^a + L \frac{d\bar{\mathbf{U}}_{j-1}}{dy} = \frac{2\mathbf{T}'L}{Et^*} \cot \alpha.$$

The solution of this last equation is

$$\left. \begin{aligned} \bar{\mathbf{U}}_j &= \frac{\mathbf{T}'y}{Et^*} \cot \alpha + \frac{j\mathbf{T}'L}{Et^*} \operatorname{cosec} \alpha + k_1, \\ \bar{\mathbf{V}}_j &= \frac{j\mathbf{T}'L}{Et^*} \cot \alpha + k_2, \end{aligned} \right\} \dots \dots \dots \dots \quad (38)$$

where k_1 and k_2 are arbitrary constants.

The elementary torsion distribution is defined by

$$\left. \begin{aligned} S_j &= S' = \text{a constant} \\ \mathbf{T}_j &= -2S' \cos \alpha \\ -S_{Rj} &= S_{Fj} = S' \\ P_{Rj} &= P_{Fj} = 0 \end{aligned} \right\} \dots \dots \dots \dots \quad (39)$$

From equations (10) and (12) it is seen that the displacement components in the skin-stringer combination are

$$\begin{aligned}\bar{\mathbf{U}}_j &= \bar{\mathbf{U}}_{j-1}, \\ \bar{\mathbf{v}}_j - \bar{\mathbf{v}}_{j-1} &= \frac{S'L}{\mu t} \sin \alpha - L \frac{d\bar{\mathbf{U}}_{j-1}}{d\mathbf{y}}\end{aligned}$$

and the boom displacements are

$$\bar{\mathbf{U}}_{Rj} = \bar{\mathbf{U}}_j(a) \quad \text{and} \quad \bar{\mathbf{U}}_{Fj} = \bar{\mathbf{U}}_j(-a).$$

From equation (33) and using equations (21), (24), (25) and (28) it follows that

$$\bar{\mathbf{v}}_j - \bar{\mathbf{v}}_{j-1} = \frac{S'Lb}{2a\mu} \left(\frac{1}{t_R} + \frac{1}{t_F} \right) + \frac{L}{2a} \left[\bar{\mathbf{U}}_{j-1} \right]_{-a}^a$$

and therefore from above

$$\frac{L}{2a} \left[\bar{\mathbf{U}}_{j-1} \right]_{-a}^a + L \frac{d\bar{\mathbf{U}}_{j-1}}{d\mathbf{y}} = \frac{S'L}{\mu t} \sin \alpha - \frac{S'Lb}{2a\mu} \left(\frac{1}{t_R} + \frac{1}{t_F} \right).$$

The solution of this last equation is

$$\left. \begin{aligned}\bar{\mathbf{U}}_j &= \left\{ \frac{S'}{2\mu t} \sin \alpha - \frac{S'b}{4a\mu} \left(\frac{1}{t_R} + \frac{1}{t_F} \right) \right\} \mathbf{y} + k_3, \\ \bar{\mathbf{v}}_j &= \left\{ \frac{S'L}{2\mu t} \sin \alpha + \frac{S'Lb}{4a\mu} \left(\frac{1}{t_R} + \frac{1}{t_F} \right) \right\} j + k_4,\end{aligned}\right\} \dots \dots \dots (40)$$

where k_3 and k_4 are arbitrary constants.

From equations (38) and (40) it is seen for both the elementary bending and torsion distributions that there is a linear warping of the ribs, the magnitude being denoted by the coefficients of \mathbf{y} in the expressions for $\bar{\mathbf{U}}_j$. This warping vanishes when the shell model contains simultaneously the elementary bending and torsion distributions such that

$$\frac{\mathbf{T}'}{S'} = - \frac{Et^* \tan \alpha}{\mu t} \left\{ \sin \alpha - \frac{1}{2} \left(\frac{b}{a} \right) \left(\frac{t}{t_R} + \frac{t}{t_F} \right) \right\}. \quad \dots \dots \dots (41)$$

The resultant of these stress distributions corresponds to a moment vector inclined at an angle† ψ from the centre-stringer (Fig. 1) where

$$\tan \psi = - \frac{\mathbf{T}'}{S'} \frac{\operatorname{cosec} \alpha}{2} \left\{ 1 + \frac{\operatorname{cosec} \alpha}{2at^*} (A_R + A_F) \right\} \quad \dots \dots \dots (42)$$

and \mathbf{T}'/S' is as given by equation (41).

The vanishing of the rib warping means of course that there is no redistribution of stress when the wing structure is built in at a rib. There will, however, be a redistribution of stress in the vicinity of the applied couple unless it is applied in a manner corresponding to the distributions given in equations (37) and (39).

† The angle ψ can readily be determined from the paper by Hemp³. From equations (35), (77) and (101) of that paper, the condition for zero warping of the ribs is that

$$\frac{\mathbf{T}'}{S'} = - \frac{\left(A_{33} - 2A_{31} \cos \alpha - \frac{b}{\mu t_R a} \right)}{A_{31}}, \quad t_R = t_F,$$

where the notation of the present paper has been retained excepting A_{31} and A_{33} which are defined by equation (33) of Hemp's paper. The angle ψ is then determined by substituting this value of \mathbf{T}'/S' into equation (42) above.

APPENDIX III

Specialisation of the Equations for the Unswept Wing

Considerable simplifications are afforded for the case of the unswept wing, *viz.*, $\alpha = 90$ deg. Symmetrical properties of the structure can then be used to good advantage, and, furthermore, the functions employed in equations (16) and (18) are then orthogonal functions. These equations become

$$\left. \begin{aligned} \bar{T}_j &= \sum_{k=1}^n \frac{C_k' \cosh \lambda_k(y/L)}{c_k' \cosh \lambda_k(y/L)} \cos \frac{\pi(2k-1)j}{2n} \\ S_j &= \frac{\mu t}{L} (\bar{v}_j - \bar{v}_{j-1}) \\ &+ \sum_{k=1}^n \frac{2}{\lambda_k} \frac{C_k' \sinh \lambda_k(y/L)}{c_k' \cosh \lambda_k(y/L)} \sin \frac{\pi(2k-1)}{4n} \sin \frac{\pi(2k-1)(2j-1)}{4n}, \end{aligned} \right\} \dots \quad (43)$$

where

$$\lambda_k = \left[\frac{6Et^*}{\mu t} \left\{ \frac{1 - \cos \frac{\pi(2k-1)}{2n}}{2 + \cos \frac{\pi(2k-1)}{2n}} \right\} \right]^{1/2}$$

The equations are exact for the shell model described in section 2, and it is readily verified for $\alpha = 90$ deg that the fundamental equations for the skin-stringer combination agree with those developed by the author¹ in a preceding paper, when the rib booms are considered inextensional. In Appendix III of that paper it was demonstrated that these fundamental equations correspond to those developed by Williams⁵ when the ribs are closely spaced. It therefore follows that equations (43) are the finite difference counterparts of the equations used by Williams², in his shear lag analysis of the unswept wing. Of course, the constants c_k' and \bar{v}_j are zero by virtue of the symmetry of the structure and loading.

For the end constraint problem of the unswept wing under torsion, Williams⁵ has shown that the chordwise variation of the shear-stress resultants S_j is small enough to be neglected. This corresponds to $C_k' = c_k' = 0$ in equations (43) and then of course the area of the spar booms must include the appropriate effective area of the skin-stringer combination. Proceeding as indicated in the body of the report will yield results identical with those of Cox⁶.

APPENDIX IV

Numerical Procedure for Evaluation of the Stress Distribution and Deflections

It can be seen on reference to the foregoing equations that the numerical work involved in their evaluation will be considerable. An analysis of the unswept wing usually requires the solution of the 'shear lag⁵ problem' presented when the wing is resisting a normal force loading, and also requires the *separate* solution of an 'end constraint⁶ problem' arising when the wing is under torsion. The analysis of the swept wing does not, however, appear to permit a comparable separation of problems. This coupled with the loss of orthogonal relations between the functions, means that the numerical work will inevitably be considerable in the corresponding calculations for a swept wing.

The following sets out in detail a suggested numerical procedure for the evaluation of the stress distribution and deflections. It has been found convenient to use matrices and the procedure has been so planned that the elements of a matrix are obtained by simple operations on the elements of preceding matrices. Having determined the values of the unknown constants (*viz.*, the V_j , C_k and c_k) these matrices then readily yield the spanwise distribution of stresses and deflections at the front and rear spars.

Appreciable numerical simplification is obtained when the ribs may be considered rigid in shear (*viz.*, $\mu\bar{t} = \infty$). This simplification will be adopted in that which follows. The procedure for ribs of finite shear rigidity is indicated.

Furthermore, the applied loading has been specialised for $W_j = M_j = 0$, $j \neq n$ (*see* Fig. 8) which corresponds to a tip force normal to the plane of the wing and a tip couple in the plane of the rib. Alternative systems of loading involve only minor modifications to the equations; all the matrices that are the coefficients of the C_k and c_k remain unchanged.

The first step is to determine the n roots λ_k of the quadratics

$$(2\lambda_k^2 - B)^2 \sin^2 \frac{\pi(2k-1)}{2n} - \lambda_k^2(6B - A^2 - 3\lambda_k^2) \cos^2 \frac{\pi(2k-1)}{2n} = 0 \quad \dots \quad (17) \text{ bis}$$

where $\lambda_k < \lambda_{n-k+1}$. These roots will be real and will fall within

$$-2\sqrt{3} \sin \alpha \left(\frac{Et^*}{\mu t} \right)^{1/2} < \lambda_k < 2\sqrt{3} \sin \alpha \left(\frac{Et^*}{\mu t} \right)^{1/2}$$

where it is necessary only to consider the positive roots. With these values it is possible to form the following basic matrices.

The direct stress resultants \bar{T}_j in the skin-stringer combination are given in equation (16) and it will be assumed that \bar{T}_n is zero. It is convenient to write the values of \bar{T}_j at $\mathbf{y} = \pm a$ in the following matrix form, *viz.*,

$$\begin{bmatrix} \bar{T}_0(a) & -\bar{T}_0(-a) \\ \bar{T}_1(a) & -\bar{T}_1(-a) \\ \dots & \dots \\ \bar{T}_{n-1}(a) & -\bar{T}_{n-1}(-a) \end{bmatrix} = \begin{bmatrix} T_{01} & T_{02} & \dots & T_{0n} \\ T_{11} & T_{12} & \dots & T_{1n} \\ \dots & \dots & \dots & \dots \\ T_{n-1,1} & T_{n-1,2} & \dots & T_{n-1,n} \end{bmatrix} \begin{bmatrix} C_1 \\ C_2 \\ \dots \\ C_n \end{bmatrix} + \begin{bmatrix} t_{01} & t_{02} & \dots & t_{0n} \\ t_{11} & t_{12} & \dots & t_{1n} \\ \dots & \dots & \dots & \dots \\ t_{n-1,1} & t_{n-1,2} & \dots & t_{n-1,n} \end{bmatrix} \begin{bmatrix} c_1 \\ c_2 \\ \dots \\ c_n \end{bmatrix}, \quad \dots \quad (44)$$

$$\begin{bmatrix} \bar{T}_0(a) + \bar{T}_0(-a) \\ \bar{T}_1(a) + \bar{T}_1(-a) \\ \dots \\ \bar{T}_{n-1}(a) + \bar{T}_{n-1}(-a) \end{bmatrix} = \begin{bmatrix} T'_{01} & T'_{02} \dots \dots T'_{0n} \\ T'_{11} & T'_{12} \dots \dots T'_{1n} \\ \dots \\ T'_{n-1,1} & T'_{n-1,2} \dots \dots T'_{n-1,n} \end{bmatrix} \begin{bmatrix} C_1 \\ C_2 \\ \dots \\ C_n \end{bmatrix} + \begin{bmatrix} t'_{01} & t'_{02} \dots \dots t'_{0n} \\ t'_{11} & t'_{12} \dots \dots t'_{1n} \\ \dots \\ t'_{n-1,1} & t'_{n-1,2} \dots \dots t'_{n-1,n} \end{bmatrix} \begin{bmatrix} c_1 \\ c_2 \\ \dots \\ c_n \end{bmatrix}, \quad \dots \quad (45)$$

The matrix elements are given by

$$T_{jk} = \{ \exp \{ \lambda_k(a/L) \} - \exp \{ - \lambda_k(a/L) \} \} \left(\frac{\lambda_k^2 + A\lambda_k + B}{\lambda_k^2 - A\lambda_k + B} \right)^{j/2} \cos \frac{\pi(2k-1)j}{2n},$$

$$t_{jk} = - \{ \exp \{ \lambda_k(a/L) \} - \exp \{ - \lambda_k(a/L) \} \} \left(\frac{\lambda_k^2 + A\lambda_k + B}{\lambda_k^2 - A\lambda_k + B} \right)^{-j/2} \cos \frac{\pi(2k-1)j}{2n},$$

$$T'_{jk} = \{ \exp \{ \lambda_k(a/L) \} + \exp \{ - \lambda_k(a/L) \} \} \left(\frac{\lambda_k^2 + A\lambda_k + B}{\lambda_k^2 - A\lambda_k + B} \right)^{j/2} \cos \frac{\pi(2k-1)j}{2n},$$

$$t'_{jk} = \{ \exp \{ \lambda_k(a/L) \} + \exp \{ - \lambda_k(a/L) \} \} \left(\frac{\lambda_k^2 + A\lambda_k + B}{\lambda_k^2 - A\lambda_k + B} \right)^{-j/2} \cos \frac{\pi(2k-1)j}{2n}.$$

Equations (44) and (45) represent the basic matrices from which all following matrices will be derived.

It is now necessary to express the displacement components \bar{V}_j of the skin-stringer combination in terms of the C_k and c_k . To this end it is necessary to express the following four quantities in matrix form. The first concerns the shear stress resultant, S_j , given in equation (18) where the values at $y = \pm a$ may be written

$$\begin{bmatrix} S_1(a) - S_1(-a) \\ S_2(a) - S_2(-a) \\ \dots \\ S_n(a) - S_n(-a) \end{bmatrix} = \begin{bmatrix} S_{11} & S_{12} \dots \dots S_{1n} \\ S_{21} & S_{22} \dots \dots S_{2n} \\ \dots \\ S_{n1} & S_{n2} \dots \dots S_{nn} \end{bmatrix} \begin{bmatrix} C_1 \\ C_2 \\ \dots \\ C_n \end{bmatrix} + \begin{bmatrix} s_{11} & s_{12} \dots \dots s_{1n} \\ s_{21} & s_{22} \dots \dots s_{2n} \\ \dots \\ s_{n1} & s_{n2} \dots \dots s_{nn} \end{bmatrix} \begin{bmatrix} c_1 \\ c_2 \\ \dots \\ c_n \end{bmatrix} \quad \dots \quad (46)$$

where, from equation (44), the elements are given by

$$S_{jk} = -\frac{1}{\lambda_k} (\mathbf{T}_{jk} - \mathbf{T}_{j-1,k}),$$

$$s_{jk} = \frac{1}{\lambda_k} (\mathbf{t}_{jk} - \mathbf{t}_{j-1,k}).$$

The next concerns the displacement components $\bar{\mathbf{U}}_j$ in the skin-stringer combination which are given in equation (10). With the aid of equation (9), this may be more conveniently expressed as

$$\bar{\mathbf{U}}_j = \frac{L \operatorname{cosec} \alpha}{2Et^*} \{\bar{\mathbf{T}}_j + \bar{\mathbf{T}}_{j-1} + 4S_j \cos \alpha\} + \bar{\mathbf{U}}_{j-1} \quad \dots \quad \dots \quad \dots \quad \dots \quad \dots \quad \dots \quad \dots \quad (47)$$

and the values at $\mathbf{y} = +a$ are written

$$\begin{bmatrix} \bar{\mathbf{U}}_1(a) - \bar{\mathbf{U}}_1(-a) \\ \bar{\mathbf{U}}_2(a) - \bar{\mathbf{U}}_2(-a) \\ \dots \dots \dots \\ \bar{\mathbf{U}}_n(a) - \bar{\mathbf{U}}_n(-a) \end{bmatrix} = \frac{L \operatorname{cosec} \alpha}{2Et^*} \begin{bmatrix} \mathbf{U}_{11} & \mathbf{U}_{12} & \dots & \dots & \mathbf{U}_{1n} \\ \mathbf{U}_{21} & \mathbf{U}_{22} & \dots & \dots & \mathbf{U}_{2n} \\ \dots & \dots & \dots & \dots & \dots \\ \mathbf{U}_{n1} & \mathbf{U}_{n2} & \dots & \dots & \mathbf{U}_{nn} \end{bmatrix} \begin{bmatrix} C_1 \\ C_2 \\ \dots \\ C_n \end{bmatrix} + \frac{L \operatorname{cosec} \alpha}{2Et^*} \begin{bmatrix} \mathbf{u}_{11} & \mathbf{u}_{12} & \dots & \dots & \mathbf{u}_{1n} \\ \mathbf{u}_{21} & \mathbf{u}_{22} & \dots & \dots & \mathbf{u}_{2n} \\ \dots & \dots & \dots & \dots & \dots \\ \mathbf{u}_{n1} & \mathbf{u}_{n2} & \dots & \dots & \mathbf{u}_{nn} \end{bmatrix} \begin{bmatrix} C_1 \\ C_2 \\ \dots \\ C_n \end{bmatrix} \quad \dots \quad (48)$$

20

where, from equations (44) and (46), it is found that the elements are given by

$$\mathbf{U}_{jk} - \mathbf{U}_{j-1,k} = \mathbf{T}_{jk} + \mathbf{T}_{j-1,k} + 4S_{jk} \cos \alpha,$$

$$\mathbf{u}_{jk} - \mathbf{u}_{j-1,k} = \mathbf{t}_{jk} + \mathbf{t}_{j-1,k} + 4s_{jk} \cos \alpha$$

where, of course, $\mathbf{U}_{0k} = \mathbf{u}_{0k} = 0$ since this refers to the root end.

The integral, along the j th bay, of the displacement \mathbf{U}_j in the skin-stringer combination is given in equations (24) and (28). With the aid of equation (9), this may be more conveniently expressed as

$$\int_0^L \mathbf{U}_j dx = \frac{L^2 \operatorname{cosec} \alpha}{6Et^*} \{\bar{\mathbf{T}}_j + 2\bar{\mathbf{T}}_{j-1} + 6S_j \cos \alpha\} + L\bar{\mathbf{U}}_{j-1} \quad \dots \quad \dots \quad \dots \quad \dots \quad \dots \quad (49)$$

and the values at $\mathbf{y} = \pm a$ are written

$$\begin{bmatrix} \int_0^L \{\mathbf{U}_1(a) - \mathbf{U}_1(-a)\} dx \\ \int_0^L \{\mathbf{U}_2(a) - \mathbf{U}_2(-a)\} dx \\ \dots \dots \dots \\ \int_0^L \{\mathbf{U}_n(a) - \mathbf{U}_n(-a)\} dx \end{bmatrix} = \frac{L^2 \operatorname{cosec} \alpha}{6Et^*} \begin{bmatrix} \mathbf{u}_{11} & \mathbf{u}_{12} & \dots & \dots & \mathbf{u}_{1n} \\ \mathbf{u}_{21} & \mathbf{u}_{22} & \dots & \dots & \mathbf{u}_{2n} \\ \dots & \dots & \dots & \dots & \dots \\ \mathbf{u}_{n1} & \mathbf{u}_{n2} & \dots & \dots & \mathbf{u}_{nn} \end{bmatrix} \begin{bmatrix} C_1 \\ C_2 \\ \dots \\ C_n \end{bmatrix} + \frac{L^2 \operatorname{cosec} \alpha}{6Et^*} \begin{bmatrix} \mathbf{u}_{11} & \mathbf{u}_{12} & \dots & \dots & \mathbf{u}_{1n} \\ \mathbf{u}_{21} & \mathbf{u}_{22} & \dots & \dots & \mathbf{u}_{2n} \\ \dots & \dots & \dots & \dots & \dots \\ \mathbf{u}_{n1} & \mathbf{u}_{n2} & \dots & \dots & \mathbf{u}_{nn} \end{bmatrix} \begin{bmatrix} C_1 \\ C_2 \\ \dots \\ C_n \end{bmatrix} \quad (50)$$

where, from equations (44), (46) and (48), it is seen that the elements are

$$u_{jk} = T_{jk} + 2T_{j-1,k} + 6S_{jk} \cos \alpha + 3U_{j-1,k},$$

$$u_{jk} = t_{jk} + 2t_{j-1,k} + 6s_{jk} \cos \alpha + 3u_{j-1,k}.$$

The fourth quantity to be written in matrix form before it is possible to express the displacements components \bar{V}_j in terms of the C_k and c_k concerns the spar shears. These are given in equation (35) which with the aid of equation (18) may be expressed in the following matrix form, *viz.*,

$$\frac{1}{2} \begin{bmatrix} S_{R1} - S_{F1} \\ S_{R2} - S_{F2} \\ \dots \\ S_{Rn} - S_{Fn} \end{bmatrix} = -\frac{M_n}{4ab} \begin{bmatrix} 1 \\ 1 \\ \dots \\ 1 \end{bmatrix} + \frac{6Et^* \sin \alpha}{BL} \begin{bmatrix} \bar{V}_1 \\ \bar{V}_2 - \bar{V}_1 \\ \dots \\ \bar{V}_n - \bar{V}_{n-1} \end{bmatrix} + \begin{bmatrix} \mathfrak{S}_{11} & \mathfrak{S}_{12} & \dots & \mathfrak{S}_{1n} \\ \mathfrak{S}_{21} & \mathfrak{S}_{22} & \dots & \mathfrak{S}_{2n} \\ \dots & \dots & \dots & \dots \\ \mathfrak{S}_{n1} & \mathfrak{S}_{n2} & \dots & \mathfrak{S}_{nn} \end{bmatrix} \begin{bmatrix} C_1 \\ C_2 \\ \dots \\ C_n \end{bmatrix} + \begin{bmatrix} s_{11} & s_{12} & \dots & s_{1n} \\ s_{21} & s_{22} & \dots & s_{2n} \\ \dots & \dots & \dots & \dots \\ s_{n1} & s_{n2} & \dots & s_{nn} \end{bmatrix} \begin{bmatrix} c_1 \\ c_2 \\ \dots \\ c_n \end{bmatrix} \dots \quad (51)$$

where, from equation (46), the elements are found to be

$$\mathfrak{S}_{jk} = \frac{1}{2} \left(\frac{L}{a} \right) \frac{1}{\lambda_k} S_{jk},$$

$$s = -\frac{1}{2} \left(\frac{L}{a} \right) \frac{1}{\lambda_k} S_{jk}.$$

It is to be noted that equation (51) is appropriate only for the applied loading $W_j = M_j = 0, j \neq n$. Other systems of applied loading modify only the first column matrix on the right-hand side. This is the case for all the following expressions.

It is now possible to express the \bar{V}_j in terms of the C_k and c_k , for from equation (33)

$$\bar{V}_j - \bar{V}_{j-1} = -\frac{Lb}{a\mu t_R} \frac{1}{2} (S_{Rj} - S_{Fj}) + \frac{1}{2a} \int_0^L \{U_j(a) - U_j(-a)\} dx$$

by virtue of equations (21) and (25) and where it is assumed that the ribs may be considered rigid in shear (i.e., $\mu t = \infty$). Substitution from equations (50) and (51) yields

$$\frac{12Et^* \sin \alpha}{BL} \begin{bmatrix} \bar{V}_1 \\ \bar{V}_2 - \bar{V}_1 \\ \dots \\ \bar{V}_n - \bar{V}_{n-1} \end{bmatrix} = \frac{H}{(1+H)} \frac{M_n}{2ab} \begin{bmatrix} 1 \\ 1 \\ \dots \\ 1 \end{bmatrix} + \begin{bmatrix} v_{11} & v_{12} & \dots & v_{1n} \\ v_{21} & v_{22} & \dots & v_{2n} \\ \dots & \dots & \dots & \dots \\ v_{n1} & v_{n2} & \dots & v_{nn} \end{bmatrix} \begin{bmatrix} C_1 \\ C_2 \\ \dots \\ C_n \end{bmatrix} + \begin{bmatrix} v_{11} & v_{12} & \dots & v_{1n} \\ v_{21} & v_{22} & \dots & v_{2n} \\ \dots & \dots & \dots & \dots \\ v_{n1} & v_{n2} & \dots & v_{nn} \end{bmatrix} \begin{bmatrix} c_1 \\ c_2 \\ \dots \\ c_n \end{bmatrix} \dots \quad (52)$$

where H is a non-dimensional structural parameter defined as

$$H = \frac{6}{B} \left(\frac{Et^*b}{\mu t_R a} \right) \sin \alpha$$

and it has been assumed that $t_F = t_R$. The elements of equation (52) are given by

$$\mathbf{v}_{jk} = - \frac{2H}{1+H} \mathfrak{C}_{jk} + \frac{1}{B} \left(\frac{L}{a} \right) \frac{1}{1+H} u_{jk} ,$$

$$s_{jk} = - \frac{2H}{1+H} \mathfrak{s}_{jk} + \frac{1}{B} \left(\frac{L}{a} \right) \frac{1}{1+H} u_{jk} .$$

When the ribs cannot be considered rigid in shear, the displacement components $\bar{\mathbf{V}}_j - \bar{\mathbf{V}}_{j-1}$ could be retained as unknowns and be determined along with the C_k, c_k from the final set of simultaneous equations (64) and (65). Alternatively, it is possible at this stage to solve the n simultaneous equations and thereby express the $\bar{\mathbf{V}}_j - \bar{\mathbf{V}}_{j-1}$ in terms of the C_k, c_k and applied loading.

Equation (52) expresses the displacement components $\bar{\mathbf{V}}_j$ in terms of the C_k and c_k and it is now necessary to write down the complementary equations to equations (46), (48) and (50). This is a necessary preliminary before determining the actual values of the C_k and c_k . Complementary to equation (46) is

$$\begin{bmatrix} S_1(a) + S_1(-a) \\ S_2(a) + S_2(-a) \\ \dots \\ S_n(a) + S_n(-a) \end{bmatrix} = \frac{H}{(1+H)} \frac{M_n}{2ab} \begin{bmatrix} 1 \\ 1 \\ \dots \\ 1 \end{bmatrix} + \begin{bmatrix} S'_{11} & S'_{12} & \dots & S'_{1n} \\ S'_{21} & S'_{22} & \dots & S'_{2n} \\ \dots & \dots & \dots & \dots \\ S'_{n1} & S'_{n2} & \dots & S'_{nn} \end{bmatrix} \begin{bmatrix} C_1 \\ C_2 \\ \dots \\ C_n \end{bmatrix} + \begin{bmatrix} s'_{11} & s'_{12} & \dots & s'_{1n} \\ s'_{21} & s'_{22} & \dots & s'_{2n} \\ \dots & \dots & \dots & \dots \\ s'_{n1} & s'_{n2} & \dots & s'_{nn} \end{bmatrix} \begin{bmatrix} c_1 \\ c_2 \\ \dots \\ c_n \end{bmatrix} \dots \quad (53)$$

where the elements are determined from equations (45) and (52) so that

$$S'_{jk} = \mathbf{v}_{jk} - \frac{1}{\lambda_k} (\mathbf{T}'_{jk} - \mathbf{T}'_{j-1,k}) ,$$

$$s'_{jk} = \mathbf{v}_{jk} + \frac{1}{\lambda_k} (\mathbf{t}'_{jk} - \mathbf{t}'_{j-1,k}) .$$

Complementary to equation (48) is

$$\begin{bmatrix} \mathbf{U}_1(a) + \mathbf{U}_1(-a) \\ \mathbf{U}_2(a) + \mathbf{U}_2(-a) \\ \dots \\ \mathbf{U}_n(a) + \mathbf{U}_n(-a) \end{bmatrix} = \frac{L \cot \alpha}{Et^*} \cdot \frac{H}{(1+H)} \frac{M_n}{ab} \begin{bmatrix} 1 \\ 2 \\ \dots \\ n \end{bmatrix} + \frac{L \operatorname{cosec} \alpha}{2Et^*} \begin{bmatrix} \mathbf{U}'_{11} & \mathbf{U}'_{12} & \dots & \mathbf{U}'_{1n} \\ \mathbf{U}'_{21} & \mathbf{U}'_{22} & \dots & \mathbf{U}'_{2n} \\ \dots & \dots & \dots & \dots \\ \mathbf{U}'_{n1} & \mathbf{U}'_{n2} & \dots & \mathbf{U}'_{nn} \end{bmatrix} \begin{bmatrix} C_1 \\ C_2 \\ \dots \\ C_n \end{bmatrix} + \frac{L \operatorname{cosec} \alpha}{2Et^*} \begin{bmatrix} \mathbf{u}'_{11} & \mathbf{u}'_{12} & \dots & \mathbf{u}'_{1n} \\ \mathbf{u}'_{21} & \mathbf{u}'_{22} & \dots & \mathbf{u}'_{2n} \\ \dots & \dots & \dots & \dots \\ \mathbf{u}'_{n1} & \mathbf{u}'_{n2} & \dots & \mathbf{u}'_{nn} \end{bmatrix} \begin{bmatrix} c_1 \\ c_2 \\ \dots \\ c_n \end{bmatrix} \quad (54)$$

where the elements are determined from equations (45) and (53) so that

$$\mathbf{U}'_{jk} - \mathbf{U}'_{j-1,k} = \mathbf{T}'_{jk} + \mathbf{T}'_{j-1,k} + 4S'_{jk} \cos \alpha,$$

$$\mathbf{u}'_{jk} - \mathbf{u}'_{j-1,k} = \mathbf{t}'_{jk} + \mathbf{t}'_{j-1,k} + 4s'_{jk} \cos \alpha$$

where, of course, $\mathbf{U}'_{0k} = \mathbf{u}'_{0k} = 0$ since this refers to the root end.

Finally, the complementary equation to equation (50) is

$$\begin{bmatrix} \int_0^L \{\mathbf{U}_1(a) + \mathbf{U}_1(-a)\} d\mathbf{x} \\ \int_0^L \{\mathbf{U}_2(a) + \mathbf{U}_2(-a)\} d\mathbf{x} \\ \dots \\ \int_0^L \{\mathbf{U}_n(a) + \mathbf{U}_n(-a)\} d\mathbf{x} \end{bmatrix} = \frac{L^2 \cot \alpha}{Et^*} \frac{H}{(1+H)} \frac{M_n}{2ab} \begin{bmatrix} 1 \\ 3 \\ \dots \\ 2n-1 \end{bmatrix} + \frac{L^2 \operatorname{cosec} \alpha}{6Et^*} \begin{bmatrix} \mathbf{u}'_{11} & \mathbf{u}'_{12} & \dots & \mathbf{u}'_{1n} \\ \mathbf{u}'_{21} & \mathbf{u}'_{22} & \dots & \mathbf{u}'_{2n} \\ \dots & \dots & \dots & \dots \\ \mathbf{u}'_{n1} & \mathbf{u}'_{n2} & \dots & \mathbf{u}'_{nn} \end{bmatrix} \begin{bmatrix} C_1 \\ C_2 \\ \dots \\ C_n \end{bmatrix} + \frac{L^2 \operatorname{cosec} \alpha}{6Et^*} \begin{bmatrix} \mathbf{u}'_{11} & \mathbf{u}'_{12} & \dots & \mathbf{u}'_{1n} \\ \mathbf{u}'_{21} & \mathbf{u}'_{22} & \dots & \mathbf{u}'_{2n} \\ \dots & \dots & \dots & \dots \\ \mathbf{u}'_{n1} & \mathbf{u}'_{n2} & \dots & \mathbf{u}'_{nn} \end{bmatrix} \begin{bmatrix} c_1 \\ c_2 \\ \dots \\ c_n \end{bmatrix} \quad (55)$$

where the elements are determined from equations (45), (53) and (54) so that

$$\mathbf{u}'_{jk} = \mathbf{T}'_{jk} + 2\mathbf{T}'_{j-1,k} + 6S'_{jk} \cos \alpha + 3\mathbf{U}'_{j-1,k},$$

$$\mathbf{u}'_{jk} = \mathbf{t}'_{jk} + 2\mathbf{t}'_{j-1,k} + 6s'_{jk} \cos \alpha + 3\mathbf{u}'_{j-1,k}.$$

It only remains now to determine the equations for the spar booms before it is possible to solve for the values of the C_k and c_k . The end loads in the spar booms are given in equations (19) and (20) so that

$$\begin{bmatrix} \bar{P}_{R0} - \bar{P}_{F0} \\ \bar{P}_{R1} - \bar{P}_{F1} \\ \dots \\ \bar{P}_{Rn-1} - \bar{P}_{Fn-1} \end{bmatrix} = L \left(\frac{1-H}{1+H} \right) \frac{M_n}{2ab} \begin{bmatrix} n \\ n-1 \\ \dots \\ 1 \end{bmatrix} + L \begin{bmatrix} P_{01} & P_{02} & \dots & P_{0n} \\ P_{11} & P_{12} & \dots & P_{1n} \\ \dots & \dots & \dots & \dots \\ P_{n-1,1} & P_{n-1,2} & \dots & P_{n-1,n} \end{bmatrix} \begin{bmatrix} C_1 \\ C_2 \\ \dots \\ C_n \end{bmatrix} + L \begin{bmatrix} \phi_{01} & \phi_{02} & \dots & \phi_{0n} \\ \phi_{11} & \phi_{12} & \dots & \phi_{1n} \\ \dots & \dots & \dots & \dots \\ \phi_{n-1,1} & \phi_{n-1,2} & \dots & \phi_{n-1,n} \end{bmatrix} \begin{bmatrix} c_1 \\ c_2 \\ \dots \\ c_n \end{bmatrix} \quad (56)$$

where, from equations (51), (52) and (53), the elements are found to be given by

$$P_{jk} - P_{j-1,k} = S'_{jk} + 2\mathfrak{S}_{jk} + \mathbf{V}_{jk} ,$$

$$p_{jk} - p_{j-1,k} = s'_{jk} + 2\mathfrak{s}_{jk} + \mathbf{v}_{jk} ,$$

and

$$\begin{bmatrix} \bar{P}_{R0} + \bar{P}_{F0} \\ \bar{P}_{R1} + \bar{P}_{F1} \\ \dots \\ \bar{P}_{Rn-1} + \bar{P}_{Fn-1} \end{bmatrix} = L \frac{W_n}{2b} \begin{bmatrix} n \\ n-1 \\ \dots \\ 1 \end{bmatrix} + L \begin{bmatrix} P'_{01} & P'_{02} & \dots & P'_{0n} \\ P'_{11} & P'_{12} & \dots & P'_{1n} \\ \dots & \dots & \dots & \dots \\ P'_{n-1,1} & P'_{n-1,2} & \dots & P'_{n-1,n} \end{bmatrix} \begin{bmatrix} C_1 \\ C_2 \\ \dots \\ C_n \end{bmatrix} + L \begin{bmatrix} p'_{01} & p'_{02} & \dots & p'_{0n} \\ p'_{11} & p'_{12} & \dots & p'_{1n} \\ \dots & \dots & \dots & \dots \\ p'_{n-1,1} & p'_{n-1,2} & \dots & p'_{n-1,n} \end{bmatrix} \begin{bmatrix} c_1 \\ c_2 \\ \dots \\ c_n \end{bmatrix} \dots \dots \quad (57)$$

where, from equation (46), the elements are found to be given by

$$P'_{jk} - P'_{j-1,k} = S_{jk} ,$$

$$p'_{jk} - p'_{j-1,k} = s_{jk} .$$

It is to be noted in the above two equations that $P_{nk} = p_{nk} = P'_{nk} = p'_{nk} = 0$ because no loads are applied to the free end of the booms.

24

The boom displacements are given in equations (22) and (26), which with the aid of equations (19 and (20) may be more conveniently expressed as

$$\left. \begin{aligned} \bar{\mathbf{U}}_{Rj} &= \frac{L}{2EA_R} (\bar{P}_{Rj} + \bar{P}_{Rj-1}) + \bar{\mathbf{U}}_{Rj-1} , \\ \bar{\mathbf{U}}_{Fj} &= \frac{L}{2EA_F} (\bar{P}_{Fj} + \bar{P}_{Fj-1}) + \bar{\mathbf{U}}_{Fj-1} \end{aligned} \right\} \dots \dots \dots \quad (58)$$

Hence, these displacements may be written

$$\begin{bmatrix} \bar{\mathbf{U}}_{R1} - \bar{\mathbf{U}}_{F1} \\ \bar{\mathbf{U}}_{R2} - \bar{\mathbf{U}}_{F2} \\ \dots \\ \bar{\mathbf{U}}_{Rj} - \bar{\mathbf{U}}_{Fj} \\ \dots \\ \bar{\mathbf{U}}_{Rn} - \bar{\mathbf{U}}_{Fn} \end{bmatrix} = \frac{L^2}{2EA_R} \left(\frac{1-H}{1+H} \right) \frac{M_n}{2ab} \begin{bmatrix} 2n-1 \\ 4n-4 \\ \dots \\ j(2n-j) \\ \dots \\ n^2 \end{bmatrix} + \frac{L^2}{2EA_R} \begin{bmatrix} \mathbf{U}_{B11} & \mathbf{U}_{B12} & \dots & \mathbf{U}_{B1n} \\ \mathbf{U}_{B21} & \mathbf{U}_{B22} & \dots & \mathbf{U}_{B2n} \\ \dots & \dots & \dots & \dots \\ \dots & \dots & \dots & \dots \\ \dots & \dots & \dots & \dots \\ \mathbf{U}_{Bn1} & \mathbf{U}_{Bn2} & \dots & \mathbf{U}_{Bnn} \end{bmatrix} \begin{bmatrix} C_1 \\ C_2 \\ \dots \\ C_n \end{bmatrix} + \frac{L^2}{2EA_R} \begin{bmatrix} \mathbf{u}_{B11} & \mathbf{u}_{B12} & \dots & \mathbf{u}_{B1n} \\ \mathbf{u}_{B21} & \mathbf{u}_{B22} & \dots & \mathbf{u}_{B2n} \\ \dots & \dots & \dots & \dots \\ \dots & \dots & \dots & \dots \\ \dots & \dots & \dots & \dots \\ \mathbf{u}_{Bn1} & \mathbf{u}_{Bn2} & \dots & \mathbf{u}_{Bnn} \end{bmatrix} \begin{bmatrix} c_1 \\ c_2 \\ \dots \\ c_n \end{bmatrix} \quad (59)$$

where it has been assumed that $A_F = A_R$ and where from equation (56) the elements are found to be given by

$$\mathbf{U}_{Bjk} - \mathbf{U}_{Bj-1,k} = P_{jk} + P_{j-1,k} ,$$

$$\mathbf{u}_{Bjk} - \mathbf{u}_{Bj-1,k} = p_{jk} + p_{j-1,k} ,$$

and

$$\begin{bmatrix} \bar{\mathbf{U}}_{R1} + \bar{\mathbf{U}}_{F1} \\ \bar{\mathbf{U}}_{R2} + \bar{\mathbf{U}}_{F2} \\ \dots \\ \bar{\mathbf{U}}_{Rj} + \bar{\mathbf{U}}_{Fj} \\ \dots \\ \bar{\mathbf{U}}_{Rn} + \bar{\mathbf{U}}_{Fn} \end{bmatrix} = \frac{L^2}{2EA_R} \frac{W_n}{2b} \begin{bmatrix} 2n-1 \\ 4n-4 \\ \dots \\ j(2n-j) \\ \dots \\ n^2 \end{bmatrix} + \frac{L^2}{2EA_R} \begin{bmatrix} \mathbf{U}'_{B11} & \mathbf{U}'_{B12} & \dots & \mathbf{U}'_{B1n} \\ \mathbf{U}'_{B21} & \mathbf{U}'_{B22} & \dots & \mathbf{U}'_{B2n} \\ \dots & \dots & \dots & \dots \\ \dots & \dots & \dots & \dots \\ \mathbf{U}'_{Bn1} & \mathbf{U}'_{Bn2} & \dots & \mathbf{U}'_{Bnn} \end{bmatrix} \begin{bmatrix} C_1 \\ C_2 \\ \dots \\ C_n \end{bmatrix} + \frac{L^2}{2EA_R} \begin{bmatrix} \mathbf{u}'_{B11} & \mathbf{u}'_{B12} & \dots & \mathbf{u}'_{B1n} \\ \mathbf{u}'_{B21} & \mathbf{u}'_{B22} & \dots & \mathbf{u}'_{B2n} \\ \dots & \dots & \dots & \dots \\ \dots & \dots & \dots & \dots \\ \mathbf{u}'_{Bn1} & \mathbf{u}'_{Bn2} & \dots & \mathbf{u}'_{Bnn} \end{bmatrix} \begin{bmatrix} C_1 \\ C_2 \\ \dots \\ C_n \end{bmatrix} \dots \quad (60)$$

where from equation (57) the elements are found to be given by

$$\mathbf{U}'_{Bjk} - \mathbf{U}'_{Bj-1,k} = P'_{jk} + P'_{j-1,k} ,$$

$$\mathbf{u}'_{Bjk} - \mathbf{u}'_{Bj-1,k} = p'_{jk} + p'_{j-1,k} .$$

It is to be noted in equations (59) and (60) that $\mathbf{U}_{B0k} = \mathbf{u}_{B0k} = \mathbf{U}'_{B0k} = \mathbf{u}'_{B0k} = 0$ since this refers to the root end.

To complete the expressions for the spar booms it is now only necessary to express in matrix form the integral of the boom displacements along each bay. These integrals are given in equations (23) and (27) which with the aid of equations (19) and (20) become

$$\left. \begin{aligned} \int_0^L \mathbf{U}_{Rj} d\mathbf{x} &= \frac{L^2}{6EA_R} (\bar{P}_{Rj} + 2\bar{P}_{Rj-1}) + L\bar{\mathbf{U}}_{Rj-1} \\ \int_0^L \mathbf{U}_{Fj} d\mathbf{x} &= \frac{L^2}{6EA_R} (\bar{P}_{Fj} + 2\bar{P}_{Fj-1}) + L\bar{\mathbf{U}}_{Fj-1} \end{aligned} \right\} \dots \dots \dots \quad (61)$$

These integrals may be expressed as

$$\begin{bmatrix} \int_0^L (\mathbf{U}_{R1} - \mathbf{U}_{F1}) d\mathbf{x} \\ \int_0^L (\mathbf{U}_{R2} - \mathbf{U}_{F2}) d\mathbf{x} \\ \dots \\ \int_0^L (\mathbf{U}_{Rj} - \mathbf{U}_{Fj}) d\mathbf{x} \\ \dots \\ \int_0^L (\mathbf{U}_{Rn} - \mathbf{U}_{Fn}) d\mathbf{x} \end{bmatrix} = \frac{L^3}{6EA_R} \left(\frac{1-H}{1+H} \right) \frac{M_n}{2ab} \begin{bmatrix} 3n-1 \\ 9n-7 \\ \dots \\ 3j(2n-j+1) - (3n+1) \\ \dots \\ 3n^2-1 \end{bmatrix}$$

26

$$+ \frac{L^3}{6EA_R} \begin{bmatrix} u_{B11} & u_{B12} \dots u_{B1n} \\ u_{B21} & u_{B22} \dots u_{B2n} \\ \dots \\ u_{Bn1} & u_{Bn2} \dots u_{Bnn} \end{bmatrix} \begin{bmatrix} C_1 \\ C_2 \\ \dots \\ C_n \end{bmatrix} + \frac{L^3}{6EA_R} \begin{bmatrix} u_{B11} & u_{B12} \dots u_{B1n} \\ u_{B21} & u_{B22} \dots u_{B2n} \\ \dots \\ u_{Bn1} & u_{Bn2} \dots u_{Bnn} \end{bmatrix} \begin{bmatrix} C_1 \\ C_2 \\ \dots \\ C_n \end{bmatrix} \dots \dots \quad (62)$$

where the elements are determined from equations (56) and (59) so that

$$u_{Bjk} = P_{jk} + 2P_{j-1,k} + 3u_{Bj-1,k} ,$$

$$u_{Bjk} = p_{jk} + 2p_{j-1,k} + 3u_{Bj-1,k} ,$$

and

$$\begin{bmatrix} \int_0^L (\mathbf{U}_{R1} + \mathbf{U}_{F1}) d\mathbf{x} \\ \int_0^L (\mathbf{U}_{R2} + \mathbf{U}_{F2}) d\mathbf{x} \\ \dots \\ \int_0^L (\mathbf{U}_{Rj} + \mathbf{U}_{Fj}) d\mathbf{x} \\ \dots \\ \int_0^L (\mathbf{U}_{Rn} + \mathbf{U}_{Fn}) d\mathbf{x} \end{bmatrix} = \frac{L^3}{6EA_R} \frac{W_n}{2b} \begin{bmatrix} 3n - 1 \\ 9n - 7 \\ \dots \\ 3j(2n - j + 1) - (3n + 1) \\ \dots \\ 3n^2 - 1 \end{bmatrix}$$

27

$$+ \frac{L^3}{6EA_R} \begin{bmatrix} u'_{B11} & u'_{B12} \dots u'_{B1n} \\ u'_{B21} & u'_{B22} \dots u'_{B2n} \\ \dots \\ \dots \\ u'_{Bn1} & u'_{Bn2} \dots u'_{Bnn} \end{bmatrix} \begin{bmatrix} C_1 \\ C_2 \\ \dots \\ \dots \\ C_n \end{bmatrix} + \frac{L^3}{6EA_R} \begin{bmatrix} u'_{B'11} & u'_{B'12} \dots u'_{B'1n} \\ u'_{B'21} & u'_{B'22} \dots u'_{B'2n} \\ \dots \\ \dots \\ u'_{B'n1} & u'_{B'n2} \dots u'_{B'nn} \end{bmatrix} \begin{bmatrix} C_1 \\ C_2 \\ \dots \\ \dots \\ C_n \end{bmatrix} \dots \dots \quad (63)$$

where the elements are determined from equations (57) and (60) so that

$$u'_{Bjk} = P'_{jk} + 2P'_{j-1,k} + 3u'_{Bj-1,k},$$

$$u'_{B'jk} = p'_{jk} + 2p'_{j-1,k} + 3u'_{B'j-1,k}.$$

It is now possible to determine the C_k and c_k by solving the $2n$ simultaneous equations presented by the relationships of equations (21) and (25). From equations (50), (55), (62) and (63) it is seen that these $2n$ simultaneous equations are

$$\begin{bmatrix} \Gamma_{11} & \Gamma_{12} & \dots & \Gamma_{1n} \\ \Gamma_{21} & \Gamma_{22} & \dots & \Gamma_{2n} \\ \dots & \dots & \dots & \dots \\ \Gamma_{j1} & \Gamma_{j2} & \dots & \Gamma_{jn} \\ \dots & \dots & \dots & \dots \\ \Gamma_{n1} & \Gamma_{n2} & \dots & \Gamma_{nn} \end{bmatrix} \begin{bmatrix} C_1 \\ C_2 \\ \dots \\ C_j \\ \dots \\ C_n \end{bmatrix} + \begin{bmatrix} \gamma_{11} & \gamma_{12} & \dots & \gamma_{1n} \\ \gamma_{21} & \gamma_{22} & \dots & \gamma_{2n} \\ \dots & \dots & \dots & \dots \\ \gamma_{j1} & \gamma_{j2} & \dots & \gamma_{jn} \\ \dots & \dots & \dots & \dots \\ \gamma_{n1} & \gamma_{n2} & \dots & \gamma_{nn} \end{bmatrix} \begin{bmatrix} c_1 \\ c_2 \\ \dots \\ c_j \\ \dots \\ c_n \end{bmatrix} = D \left(\frac{1-H}{1+H} \right) \frac{M_n}{2ab} \begin{bmatrix} 3n-1 \\ 9n-7 \\ \dots \\ 3j(2n-j+1) - (3n+1) \\ \dots \\ 3n^2-1 \end{bmatrix} \dots \dots \quad (64)$$

where D is a non-dimensional structural parameter defined as

$$D = \left(\frac{Lt^*}{A_R} \right) \sin \alpha$$

and the elements are given by

$$\begin{aligned} \Gamma_{jk} &= u_{jk} - DU_{Bjk} , \\ \gamma_{jk} &= u_{jk} - Du_{Bjk} , \end{aligned}$$

with the remaining n equations

$$\begin{bmatrix} \Gamma'_{11} & \Gamma'_{12} & \dots & \Gamma'_{1n} \\ \Gamma'_{21} & \Gamma'_{22} & \dots & \Gamma'_{2n} \\ \dots & \dots & \dots & \dots \\ \Gamma'_{j1} & \Gamma'_{j2} & \dots & \Gamma'_{jn} \\ \dots & \dots & \dots & \dots \\ \Gamma'_{n1} & \Gamma'_{n2} & \dots & \Gamma'_{nn} \end{bmatrix} \begin{bmatrix} C_1 \\ C_2 \\ \dots \\ C_j \\ \dots \\ C_n \end{bmatrix} + \begin{bmatrix} \gamma'_{11} & \gamma'_{12} & \dots & \gamma'_{1n} \\ \gamma'_{21} & \gamma'_{22} & \dots & \gamma'_{2n} \\ \dots & \dots & \dots & \dots \\ \gamma'_{j1} & \gamma'_{j2} & \dots & \gamma'_{jn} \\ \dots & \dots & \dots & \dots \\ \gamma'_{n1} & \gamma'_{n2} & \dots & \gamma'_{nn} \end{bmatrix} \begin{bmatrix} c_1 \\ c_2 \\ \dots \\ c_j \\ \dots \\ c_n \end{bmatrix} = D \frac{W_n}{2b} \begin{bmatrix} 3n-1 \\ 9n-7 \\ \dots \\ 3j(2n-j+1) - (3n+1) \\ \dots \\ 3n^2-1 \end{bmatrix} - \frac{AH}{(1+H)} \frac{M_n}{4ab} \begin{bmatrix} 1 \\ 3 \\ \dots \\ 2j-1 \\ \dots \\ 2n-1 \end{bmatrix} \dots \dots \quad (65)$$

where the elements are given by

$$\Gamma'_{jk} = u'_{jk} - D u'_{Bjk} ,$$

$$\gamma'_{jk} = u'_{jk} - D u'_{Bjk} .$$

With these values of the C_k and c_k the spanwise distribution of stresses and displacements at the front and rear spars may be obtained by simple matrix multiplication. The chordwise distributions of such as the resultants \bar{T}_j and S_j are obtained by evaluating equations (16) and (18) for various values of (y/L).

APPENDIX V

Numerical Illustrative Example

The numerical illustrative example is based on the swept wing structure shown in Fig. 9. This wing has a sweepback of 45 deg and has five bays. The loading cases of tip force normal to the plane of the wing and tip couple in the plane of the rib will be investigated where $W_5 = 100$ lb and $M_5 = 1,000$ in. lb. The following values of the non-dimensional structural parameters were taken, *viz.*,

$$A = 12 \cos \alpha = 8.5 ,$$

$$B = 6 \left(\frac{Et^*}{\mu t} \sin^2 \alpha + 4 \cos^2 \alpha \right) = 26 ,$$

$$H = \frac{6}{B} \left(\frac{Et^*}{\mu t_R a} \right) \sin \alpha = 0.17 ,$$

$$D = \left(\frac{Lt^*}{A_R} \right) \sin \alpha = 2.8 ,$$

and the ribs are considered stiff enough to be taken as rigid in shear.

As stated earlier, the numerical work is inevitably considerable for the swept wing. This necessitates working to a fairly large number of significant figures so as to ensure results that are not influenced by loss of figures due to rounding off errors and possible ill-conditioning. The following calculations were undertaken on a standard ten-bank electric calculating machine. Of course, once the values of the constants C_k and c_k have been obtained it is not necessary to retain all these significant figures.

The roots λ_k ($k = 1, 2, 3, 4$ and 5) are determined from the three quadratic equations

$$(2\lambda_k^2 - B)^2 \sin^2 \frac{\pi(2k-1)}{2n} - \lambda_k^2 (6B - A^2 - 3\lambda_k^2) \cos^2 \frac{\pi(2k-1)}{2n} = 0 \quad \dots \quad (17)\text{bis}$$

for $k = 1, 2$ and 3 . Only the positive roots are considered and these are arranged in order of increasing magnitude so that

$$[\lambda_k] = \begin{bmatrix} 0.880 & 387 & 296 \\ 2.418 & 837 & 187 \\ 3.605 & 551 & 27 \\ 4.548 & 936 & 43 \\ 5.187 & 010 & 61 \end{bmatrix}$$

It is now possible to form the first four matrices given in equations (44) and (45). They are

$$[\mathbf{T}_{jk}] = \begin{bmatrix} 2.331\ 120\ 22 & 15.271\ 709\ 87 & 58.526\ 180\ 2 & 169.792\ 534\ 7 & 348.915\ 585 \\ 2.954\ 391\ 93 & 19.340\ 046\ 02 & 0 & -325.453\ 134 & -1,100.721\ 44 \\ 3.349\ 010\ 72 & -21.906\ 466\ 7 & -488.001\ 247 & -557.960\ 323 & 3,105.842\ 84 \\ 3.242\ 460\ 48 & -145.260\ 471\ 6 & 0 & 5,599.876\ 62 & -7,484.990\ 42 \\ 2.271\ 618\ 94 & -266.225\ 666 & 4069.037\ 41 & -15,533.916\ 20 & 13,052.859\ 38 \end{bmatrix}$$

30

$$[\mathbf{t}_{jk}] = \begin{bmatrix} -2.331\ 120\ 22 & -15.271\ 709\ 87 & -58.526\ 180\ 2 & -169.792\ 534\ 7 & -348.915\ 585 \\ -1.663\ 695\ 667 & -4.166\ 344\ 67 & 0 & 30.604\ 556\ 9 & 100.040\ 525 \\ -1.062\ 008\ 74 & 1.016\ 641\ 24 & 7.019\ 067\ 66 & 4.933\ 993\ 74 & -25.655\ 267\ 6 \\ -0.579\ 017\ 943 & 1.452\ 247\ 134 & 0 & -4.656\ 626\ 18 & 5.619\ 360\ 04 \\ -0.228\ 432\ 866 & 0.573\ 377\ 563 & -0.841\ 799\ 527 & 1.214\ 706\ 94 & -0.890\ 635\ 098 \end{bmatrix}$$

$$[\mathbf{T}'_{jk}] = \begin{bmatrix} 3.071\ 501\ 50 & 15.402\ 114\ 21 & 58.560\ 343\ 0 & 169.804\ 313\ 3 & 348.921\ 317 \\ 3.892\ 728\ 99 & 19.505\ 189\ 67 & 0 & -325.475\ 710 & -1,100.739\ 522 \\ 4.412\ 681\ 68 & -22.093\ 524\ 9 & -488.286\ 102 & -557.999\ 029 & 3,105.893\ 86 \\ 4.272\ 290\ 26 & -146.500\ 843\ 2 & 0 & 5,600.265\ 09 & -7,485.113\ 38 \\ 2.993\ 102\ 17 & -268.498\ 953 & 4,071.412\ 58 & -15,534.993\ 79 & 13,053.073\ 8 \end{bmatrix}$$

$$[\mathbf{t}'_{jk}] = \begin{bmatrix} 3.071\ 501\ 50 & 15.402\ 114\ 21 & 58.560\ 343\ 0 & 169.804\ 313 & 348.921\ 317 \\ 2.192\ 097\ 90 & 4.201\ 920\ 88 & 0 & -30.606\ 680\ 0 & -100.042\ 169 \\ 1.399\ 310\ 69 & -1.025\ 322\ 28 & -7.023\ 164\ 82 & -4.934\ 336\ 02 & 25.655\ 689\ 1 \\ 0.762\ 918\ 388 & -1.464\ 647\ 80 & 0 & 4.656\ 949\ 22 & -5.619\ 452\ 36 \\ 0.300\ 984\ 860 & -0.578\ 273\ 604 & 0.842\ 290\ 900 & -1.214\ 791\ 21 & 0.890\ 649\ 730 \end{bmatrix}$$

and these are the basic matrices from which all subsequent matrices are derived by successive addition and multiplication of the elements. Including the final set of simultaneous equations there are 32 of these matrices.

The simultaneous equations for the determination of the C_k and c_k are given by equations (64) and (65). For the five bay structure under consideration there will be ten of these simultaneous equations and the coefficients for the left-hand side are eventually found to be

$$\begin{array}{l}
 [T_{jk}] = \begin{bmatrix} 152.672\ 235\ 6 & -557.988\ 969 & 4,490.600\ 80 & -9,317.816\ 65 & 6,796.349\ 09 \\ 470.950\ 334 & -1,716.223\ 076 & 12,552.007\ 07 & -31,266.189\ 2 & 15,545.857\ 03 \\ 790.625\ 966 & -3,517.547\ 84 & 17,020.854\ 88 & -50,607.534\ 4 & 39,822.975\ 6 \\ 1,073.842\ 563 & -6,961.570\ 249 & 28,200.140\ 7 & -45,659.949\ 7 & 21,015.025\ 1 \\ 1,262.172\ 432 & -11,580.717\ 01 & 69,336.973\ 2 & -161,540.098\ 9 & 103,218.605\ 7 \end{bmatrix}, \\
 \\
 [Y_{jk}] = \begin{bmatrix} -59.594\ 649\ 3 & -82.053\ 729\ 7 & -178.305\ 450\ 1 & -376.013\ 430 & -645.584\ 450 \\ -157.002\ 850\ 9 & -151.204\ 591\ 6 & -219.069\ 306 & -300.165\ 226 & -343.402\ 897 \\ -222.304\ 690 & -144.419\ 694\ 8 & -163.084\ 500\ 5 & -251.209\ 211 & -417.812\ 714 \\ -259.443\ 469 & -126.357\ 642\ 2 & -158.542\ 107\ 7 & -278.058\ 098 & -406.434\ 134 \\ -274.457\ 657 & -118.440\ 058\ 1 & -165.340\ 991\ 1 & -274.268\ 999 & -408.410\ 312 \end{bmatrix}, \\
 \\
 [T'_{jk}] = \begin{bmatrix} 31.311\ 422\ 9 & 106.518\ 443\ 1 & 297.442\ 633 & 530.510\ 42 & 632.647\ 953 \\ 106.966\ 424\ 7 & 349.375\ 305 & 227.047\ 469 & -1,547.538\ 34 & -3,228.694\ 98 \\ 199.970\ 831\ 6 & 216.062\ 075 & -3,384.440\ 90 & -2,441.459\ 12 & 8,294.348\ 69 \\ 301.362\ 303 & -1,248.998\ 448 & -2,798.025\ 37 & 23,081.582\ 8 & -21,928.042\ 5 \\ 393.203\ 716 & -4,340.930\ 08 & 27,314.627\ 6 & -65,258.009\ 4 & 41,966.956\ 4 \end{bmatrix}, \\
 \\
 [Y'_{jk}] = \begin{bmatrix} 24.302\ 383\ 9 & 54.695\ 054\ 4 & 135.618\ 456\ 0 & 302.476\ 766 & 533.894\ 048 \\ 61.079\ 721\ 4 & 90.324\ 817\ 9 & 143.994\ 854\ 0 & 197.405\ 769\ 0 & 215.491\ 945 \\ 82.256\ 007\ 2 & 75.020\ 527\ 4 & 91.991\ 546\ 6 & 156.754\ 303\ 2 & 291.645\ 519 \\ 91.770\ 994\ 7 & 58.979\ 109\ 5 & 90.920\ 840\ 3 & 181.091\ 957\ 4 & 276.507\ 444 \\ 93.426\ 255\ 1 & 53.508\ 003\ 1 & 97.091\ 495\ 6 & 175.943\ 648\ 6 & 277.859\ 645 \end{bmatrix}.
 \end{array}$$

Hence the ten simultaneous equations are

$$[I_{jk}][C_k] + [\gamma_{jk}][c_k] = \begin{bmatrix} 1.071\ 155\ 935 \\ 2.907\ 423\ 251 \\ 4.284\ 623\ 738 \\ 5.202\ 757\ 397 \\ 5.661\ 824\ 226 \end{bmatrix} M_5$$

and

$$[I'_{jk}][C_k] + [\gamma'_{jk}][c_k] = \begin{bmatrix} 13.634\ 782\ 61 \\ 37.008\ 695\ 65 \\ 54.539\ 130\ 43 \\ 66.226\ 086\ 95 \\ 72.069\ 565\ 21 \end{bmatrix} W_5 - \begin{bmatrix} 0.023\ 786\ 272\ 52 \\ 0.071\ 358\ 817\ 56 \\ 0.118\ 931\ 362\ 6 \\ 0.166\ 503\ 907\ 6 \\ 0.214\ 076\ 452\ 7 \end{bmatrix} M_5.$$

These equations were solved by the method of pivotal condensation, the pivots being chosen such that the loss of leading figures was reduced to a minimum. The values of the C_k, c_k were then found to be

	$W_5 = 100\text{ lb}$ $M_5 = 0$	$W_5 = 0$ $M_5 = 1,000\text{ in. lb}$
$C_1 =$	14.132 3	3.601 0
$C_2 =$	1.145 41	0.329 65
$C_3 =$	0.199 292	0.058 592
$C_4 =$	0.062 274	0.018 635 8
$C_5 =$	0.031 955	0.009 607 2
$c_1 =$	47.835	-11.741 7
$c_2 =$	-21.367	6.047 5
$c_3 =$	10.999 4	-4.495 5
$c_4 =$	-4.112 9	1.966 55
$c_5 =$	0.833 45	-0.441 35

With these values of the C_k, c_k it is possible to obtain the complete stress distribution and displacement pattern throughout the entire shell model. The chordwise distributions are obtained by substituting these values into the expressions such as equations (16) and (18), while the spanwise distributions at the front and rear spars may be obtained by evaluating the appropriate matrices 44 to 63. These distributions are shown plotted in Figs. 10 to 21. Panoramic views of the direct stresses along the stringers and spar booms are given in Fig. 22 which shows clearly the build up of stress towards the rear spar at the root.

It is of interest to calculate the direction ψ of the vector couple that gives zero warping of the ribs together with the resulting stresses. From equation (41) and Fig. 9 it is soon found that

$$\frac{T'}{S'} = -1.26$$

and then from equation (42) that

$$\psi = 49 \text{ deg, } 30 \text{ min.}$$

When the vector couple is of magnitude 1,000 in. lb it is easy to determine that the shear stress is

$$\frac{S'}{t} = -\frac{1,000 \cos \psi}{8abt \sin \alpha} = -71 \text{ lb/in.}^2$$

and the direct stress in the skin-stringer combination and booms is

$$\frac{T' \operatorname{cosec} \alpha}{t^*} = \left(\frac{S'}{t}\right) \left(\frac{t}{t^*}\right) \left(\frac{T'}{S'}\right) \operatorname{cosec} \alpha = 76 \text{ lb/in.}^2$$

APPENDIX VI

Tests on a Cellulose-Nitrate Model Swept Wing

To obtain some confirmation of the theoretical results the cellulose-nitrate model shown in Fig. 23 was constructed and then tested in the rig shown in Fig. 24.

The model was made from cellulose-nitrate primarily because of the simplicity and speed of construction. It served to establish a rapid qualitative confirmation of the theoretical results. This confirmation cannot be regarded quantitatively because of the following reasons, *viz.*,

- (a) the test conditions were not controlled with respect to temperature and humidity
- (b) it is difficult to obtain precise values of the elastic constants
- (c) there is change of elastic properties subsequent to glueing
- (d) the cellulose-nitrate model does not correspond precisely to the swept wing chosen for the numerical example (compare Figs. 9 and 22).

The root of the model was filled with a hard wood and then securely clamped between two massive steel plates. In this way a really rigid root end fitting was obtained. Another hard wood block was fitted to the tip so that the various loads could be applied through a pin.

The stringers and booms were laminated from 0.125-in. thick sheet and separate experiments on test coupons indicated that the following are representative values of the elastic constants, *viz.*,

$$E_{\text{sheet}} = 3.6 \times 10^5 \text{ lb/in.}^2,$$

$$E_{\text{stringer}} = 2.8 \times 10^5 \text{ lb/in.}^2,$$

$$E_{\text{boom}} = 2.8 \times 10^5 \text{ lb/in.}^2,$$

$$\text{Poisson's ratio} = 0.4.$$

The strain gauge results were converted to stresses by multiplying by the appropriate value of the elastic constant and these stresses are shown plotted in Figs. 10, 12, 13, 14, 16, 18, 19 and 20. The direct stresses refer to the skin outer fibres while the shear stresses refer to the skin middle fibres and the two sets of experimental results on each graph correspond to reversed loadings. Full details of the tests are given in a separate paper⁸.

Agreement is quite good between the theoretical and experimental results. The model has a slightly lower flexural rigidity than that taken for the numerical example, this difference is the most prominent when comparing the deflections for tip shear loading in Fig. 15. There are, of course, essential differences in the character of the stress distribution at the tip—especially for the case of the tip couple in the plane of the rib. On the model the tip is effectively 'built in' whereas for the numerical example the tip is in a free condition. As the couple is applied through the rib, the free end condition involves a local stress diffusion problem until the spar booms are carrying their proper complement of load.

Readings of the spar deflections were taken at each rib station and these are shown plotted in Figs. 15 and 21.

APPENDIX VII

Solution of the Fundamental Equations for the Skin-Stringer Combination when the Rib Flanges are Inextensional

When the rib flanges are inextensional, equations (13), (14) and (15) become

$$\left(2L^2 \frac{d^2}{dy^2} - B\right) \bar{T}_0 + \left(L^2 \frac{d^2}{dy^2} - AL \frac{d}{dy} + B\right) \bar{T}_1 = 0,$$

$$\left(L^2 \frac{d^2}{dy^2} + AL \frac{d}{dy} + B\right) \bar{T}_{j-1} + 2\left(2L^2 \frac{d^2}{dy^2} - B\right) \bar{T}_j + \left(L^2 \frac{d^2}{dy^2} - AL \frac{d}{dy} + B\right) \bar{T}_{j+1} = 0$$

and

$$\left(L^2 \frac{d^2}{dy^2} + AL \frac{d}{dy} + B\right) \bar{T}_{n-2} + 2\left(2L^2 \frac{d^2}{dy^2} - B\right) \bar{T}_{n-1} = -B\bar{T}_n$$

when \bar{T}_n is assumed constant.

It is readily observed that the particular integral of the above set of simultaneous differential equations is

$$\bar{T}_j = \bar{T}_n \text{ for } \bar{T}_n \text{ constant,}$$

and it is necessary only to determine the complementary function.

Now, it is assumed that a constituent of the complementary function is $e^{\lambda(y/L)}$ where λ is a constant. The condition of consistency for the foregoing equations then becomes

$$\begin{vmatrix} 2\lambda^2 - B & \lambda^2 - A\lambda + B & 0 & \dots & 0 & 0 \\ \lambda^2 + A\lambda + B & 2(2\lambda^2 - B) & \lambda^2 - A\lambda + B & \dots & 0 & 0 \\ 0 & \lambda^2 + A\lambda + B & 2(2\lambda^2 - B) & \dots & 0 & 0 \\ \dots & \dots & \dots & \dots & \dots & \dots \\ 0 & 0 & 0 & \dots & \lambda^2 + A\lambda + B & 2(2\lambda^2 - B) \end{vmatrix} = \Delta_n(\lambda) = 0$$

which is an $n \times n$ determinant. The relationship between successive determinants is found to be

$$\Delta_{m+2}(\lambda) - 2(2\lambda^2 - B)\Delta_{m+1}(\lambda) + (\lambda^2 - A\lambda + B)(\lambda^2 + A\lambda + B)\Delta_m(\lambda) = 0,$$

and this finite difference equation has the solution

$$\Delta_n(\lambda) = \{2\lambda^2 - B + \lambda(3\lambda^2 + A^2 - 6B)^{1/2}\}^n + \{2\lambda^2 - B - \lambda(3\lambda^2 + A^2 - 6B)^{1/2}\}^n = 0.$$

This is an expansion of the condition of consistency which may be rewritten

$$\{(2\lambda^2 - B) + \lambda(3\lambda^2 + A^2 - 6B)^{1/2}\}^n - \{(2\lambda^2 - B) - \lambda(3\lambda^2 + A^2 - 6B)^{1/2}\}^n \exp\{i\pi(2k - 1)\} = 0$$

for k integer and $i = \sqrt{-1}$. Using de Moivre's theorem,

$$\{(2\lambda^2 - B) + \lambda(3\lambda^2 + A^2 - 6B)^{1/2}\} - \{(2\lambda^2 - B) - \lambda(3\lambda^2 + A^2 - 6B)^{1/2}\} \exp\{i\pi(2k-1)/n\} = 0$$

where $k = 1, 2, 3, \dots, n$. Thus the condition of consistency in product form becomes

$$\Delta_n(\lambda) = \prod_{k=1}^n \left[(2\lambda_k^2 - B) \sin \frac{\pi(2k-1)}{2n} \pm \lambda_k(6B - A^2 - 3\lambda_k^2)^{1/2} \cos \frac{\pi(2k-1)}{2n} \right] = 0,$$

where either the positive or the negative sign is retained throughout the complete product. The significance of this is that it is not yet possible to distinguish between the λ_k th and λ_{n-k+1} th roots. Thus the roots may be determined from the quadratics

$$(2\lambda_k^2 - B)^2 \sin^2 \frac{\pi(2k-1)}{2n} - \lambda_k^2(6B - A^2 - 3\lambda_k^2) \cos^2 \frac{\pi(2k-1)}{2n} = 0$$

and they fall within $-2\sqrt{3} \sin \alpha \left(\frac{Et^*}{\mu t} \right)^{1/2} < \lambda_k < 2\sqrt{3} \sin \alpha \left(\frac{Et^*}{\mu t} \right)^{1/2}$.

Consider now the difference equations arising from (13), (14) and (15). They are

$$(2\lambda_k^2 - B)\bar{\mathbf{T}}_0 + (\lambda_k^2 - A\lambda_k + B)\bar{\mathbf{T}}_1 = 0,$$

$$(\lambda_k^2 + A\lambda_k + B)\bar{\mathbf{T}}_{j-1} + 2(2\lambda_k^2 - B)\bar{\mathbf{T}}_j + (\lambda_k^2 - A\lambda_k + B)\bar{\mathbf{T}}_{j+1} = 0$$

and

$$(\lambda_k^2 + A\lambda_k + B)\bar{\mathbf{T}}_{n-2} + 2(2\lambda_k^2 - B)\bar{\mathbf{T}}_{n-1} = 0.$$

Using the substitution

$$(2\lambda_k^2 - B) = \{(\lambda_k^2 + A\lambda_k + B)(\lambda_k^2 - A\lambda_k + B)\}^{1/2} \cos \frac{\pi(2k-1)}{2n}$$

from above, the solution of these difference equations is readily found to be

$$\bar{\mathbf{T}}_j = (-)^j \left(\frac{\lambda_k^2 + A\lambda_k + B}{\lambda_k^2 - A\lambda_k + B} \right)^{j/2} \cos \frac{\pi(2k-1)j}{2n},$$

or since the roots λ_k and λ_{n-k+1} cannot as yet be distinguished, this may be more conveniently written

$$\bar{\mathbf{T}}_j = \left(\frac{\lambda_k^2 + A\lambda_k + B}{\lambda_k^2 - A\lambda_k + B} \right)^{j/2} \cos \frac{\pi(2k-1)j}{2n}.$$

By inspection, it is found that this latter solution is applicable only when $\lambda_k < \lambda_{n-k+1}$.

Finally, the complete solution to the fundamental equations (13), (14) and (15) may therefore be written

$$\bar{\mathbf{T}}_j = \bar{\mathbf{T}}_n + \sum_{k=1}^n C_k \exp\{\lambda_k(\mathbf{y}/L)\} \left(\frac{\lambda_k^2 + A\lambda_k + B}{\lambda_k^2 - A\lambda_k + B} \right)^{j/2} \cos \frac{\pi(2k-1)j}{2n} \\ + \sum_{k=1}^n c_k \exp\{-\lambda_k(\mathbf{y}/L)\} \left(\frac{\lambda_k^2 + A\lambda_k + B}{\lambda_k^2 - A\lambda_k + B} \right)^{-j/2}$$

where C_k and c_k are arbitrary constants.

When the rib booms are extensional it is necessary to solve a set of simultaneous differential equations each of fourth order.

APPENDIX VIII

*That the Equations of Compatibility are Consistent with the
Strain Energy being Rendered a Minimum*

It is now the purpose to demonstrate by using the Calculus of Variations that the foregoing procedure is consistent with the total strain energy stored in the structure being rendered a minimum.

The total strain energy stored in the skin-stringer combination forming the top and bottom surfaces of the shell model is

$$U_s = \sum_{j=1}^n \int_{-a}^a \left\{ \frac{L}{\mu t} S_j^2 + \frac{1}{Et^*} \int_0^L T_j^2 d\mathbf{x} \right\} d\mathbf{y} \sin \alpha.$$

On substitution from equations (4) and (9) and performing the integration with respect to \mathbf{x} this becomes

$$\begin{aligned} U_s = \sum_{j=1}^n \int_{-a}^a & \left[\frac{L}{\mu t} S_j^2 + \frac{1}{Et^*} \left\{ \frac{L^3}{3} \left(\frac{dS_j}{d\mathbf{y}} \right)^2 \operatorname{cosec}^2 \alpha + L \bar{\mathbf{T}}_{j-1}^2 \operatorname{cosec}^2 \alpha \right. \right. \\ & - L^2 \bar{\mathbf{T}}_{j-1} \frac{dS_j}{d\mathbf{y}} \operatorname{cosec}^2 \alpha + 4LS_j^2 \cot^2 \alpha - 2L^2 S_j \frac{dS_j}{d\mathbf{y}} \cot \alpha \operatorname{cosec} \alpha \\ & \left. \left. + 4LS_j \bar{\mathbf{T}}_{j-1} \cot \alpha \operatorname{cosec} \alpha \right\} \right] d\mathbf{y} \sin \alpha. \end{aligned}$$

The stress resultants $\bar{\mathbf{T}}_j$ and S_j are related by virtue of equation (9). Thus, when considering an arbitrary variation of U_s it is necessary to impose the restraint

$$U_U = \sum_{j=1}^n \int_{-a}^a 2\bar{\mathbf{U}}_j(\mathbf{y}) \left(L \frac{dS_j}{d\mathbf{y}} + \bar{\mathbf{T}}_j - \bar{\mathbf{T}}_{j-1} \right) d\mathbf{y}$$

where $\bar{\mathbf{U}}_j(\mathbf{y})$ is an undetermined function which cannot as yet be associated with its interpretation as a displacement component. An arbitrary variation of the strain energy stored in the skin-stringer combination can eventually be written

$$\begin{aligned} \Delta U_s + \Delta U_U = \sum_{j=1}^n \int_{-a}^a & \left[\frac{2L}{\mu t} S_j \delta S_j \sin \alpha + \frac{1}{Et^*} \left\{ - \frac{2L^3}{3} \frac{d^2 S_j}{d\mathbf{y}^2} \delta S_j \operatorname{cosec} \alpha \right. \right. \\ & + 2L \bar{\mathbf{T}}_{j-1} \delta \bar{\mathbf{T}}_{j-1} \operatorname{cosec} \alpha + L^2 \frac{d\bar{\mathbf{T}}_{j-1}}{d\mathbf{y}} \delta S_j \operatorname{cosec} \alpha - L^2 \frac{dS_j}{d\mathbf{y}} \delta \bar{\mathbf{T}}_{j-1} \operatorname{cosec} \alpha \\ & \left. + 8LS_j \delta S_j \cot \alpha \cos \alpha + 4LS_j \delta \bar{\mathbf{T}}_{j-1} \cot \alpha + 4L \bar{\mathbf{T}}_{j-1} \delta S_j \cot \alpha \right\} \\ & + 2 \left(-L \frac{d\bar{\mathbf{U}}_j}{d\mathbf{y}} \delta S_j + \bar{\mathbf{U}}_j \delta \bar{\mathbf{T}}_j - \bar{\mathbf{U}}_j \delta \bar{\mathbf{T}}_{j-1} \right) \Big] d\mathbf{y} \\ & + \sum_{j=1}^n \left[\frac{1}{Et^*} \left(\frac{2L^3}{3} \frac{dS_j}{d\mathbf{y}} \delta S_j \operatorname{cosec} \alpha - L^2 \bar{\mathbf{T}}_{j-1} \delta S_j \operatorname{cosec} \alpha \right. \right. \\ & \left. \left. - 2L^2 S_j \delta S_j \cot \alpha \right) + 2L \bar{\mathbf{U}}_j \delta S_j \right]_{-a}^a. \end{aligned}$$

The total strain energy stored in the four spar booms is

$$U_B = \sum_{j=1}^n \int_0^L \left(\frac{P_{Rj}^2}{EA_R} + \frac{P_{Fj}^2}{EA_F} \right) d\mathbf{x}.$$

On substitution from equations (19) and (20) and performing the integration with respect to \mathbf{x} this becomes

$$U_B = \sum_{j=1}^n \frac{1}{EA_R} \left[\frac{L^3}{3} \{S_{Rj}^2 + S_j^2(a) + 2S_{Rj}S_j(a)\} + L\bar{P}_{Rj-1}^2 + L^2\bar{P}_{Rj-1} \{S_{Rj} + S_j(a)\} \right] \\ + \sum_{j=1}^n \frac{1}{EA_F} \left[\frac{L^3}{3} \{S_{Fj}^2 + S_j^2(-a) - 2S_{Fj}S_j(-a)\} + L\bar{P}_{Fj-1}^2 + L^2\bar{P}_{Fj-1} \{S_{Fj} - S_j(-a)\} \right].$$

The shear-stress resultants and boom end loads are related by virtue of equations (19) and (20). Thus, when considering an arbitrary variation of U_B it is necessary to impose the restraints

$$U_{U_{R,F}} = \sum_{j=1}^n 2\bar{U}_{Rj} [\bar{P}_{Rj} - \bar{P}_{Rj-1} - L\{S_{Rj} + S_j(a)\}] \\ + \sum_{j=1}^n 2\bar{U}_{Fj} [\bar{P}_{Fj} - \bar{P}_{Fj-1} - L\{S_{Fj} - S_j(-a)\}]$$

where \bar{U}_{Rj} and \bar{U}_{Fj} are undetermined multipliers which cannot as yet be associated with their interpretations as displacements. An arbitrary variation of the strain energy stored in the four spar booms can now be written

$$\Delta U_B + \Delta U_{U_{R,F}} = \sum_{j=1}^n \frac{1}{EA_R} \left[\frac{L^3}{3} \{2S_{Rj} \delta S_{Rj} + 2S_j(a) \delta S_j(a) + 2S_{Rj} \delta S_j(a) + 2S_j(a) \delta S_{Rj}\} \right. \\ \left. + 2L\bar{P}_{Rj-1} \delta \bar{P}_{Rj-1} + L^2\bar{P}_{Rj-1} \{\delta S_{Rj} + \delta S_j(a)\} + L^2\{S_{Rj} + S_j(a)\} \delta \bar{P}_{Rj-1} \right] \\ + \sum_{j=1}^n \frac{1}{EA_F} \left[\frac{L^3}{3} \{2S_{Fj} \delta S_{Fj} + 2S_j(-a) \delta S_j(-a) - 2S_{Fj} \delta S_j(-a) - 2S_j(-a) \delta S_{Fj}\} \right. \\ \left. + 2L\bar{P}_{Fj-1} \delta \bar{P}_{Fj-1} + L^2\bar{P}_{Fj-1} \{\delta S_{Fj} - \delta S_j(-a)\} + L^2\{S_{Fj} - S_j(-a)\} \delta \bar{P}_{Fj-1} \right] \\ + \sum_{j=1}^n 2\bar{U}_{Rj} [\delta \bar{P}_{Rj} - \delta \bar{P}_{Rj-1} - L\{\delta S_{Rj} + \delta S_j(a)\}] \\ + \sum_{j=1}^n 2\bar{U}_{Fj} [\delta \bar{P}_{Fj} - \delta \bar{P}_{Fj-1} - L\{\delta S_{Fj} - \delta S_j(-a)\}].$$

The total strain energy stored in the front and rear spar webs in shear is

$$U_W = \sum_{j=1}^n \left(\frac{LbS_{Rj}^2}{\mu t_R} + \frac{LbS_{Fj}^2}{\mu t_F} \right)$$

and subjecting this to an arbitrary variation,

$$\Delta U_W = \sum_{j=1}^n \left(\frac{2Lb}{\mu t_R} S_{Rj} \delta S_{Rj} + \frac{2Lb}{\mu t_F} S_{Fj} \delta S_{Fj} \right).$$

The total strain energy stored in the ribs in shear is given by

$$U_R = \sum_{j=1}^n \frac{2ab}{\mu \bar{t}} \bar{S}_j^2$$

where \bar{S}_j is given by equation (36). The appropriate restraint on the variation of U_R is therefore

$$U_V = \sum_{j=1}^n 4a \bar{V}_j \left\{ \frac{1}{2a} \int_{-a}^a (S_{j+1} - S_j) d\mathbf{y} + \frac{M_j}{8ab} - \bar{S}_j \right\}$$

where \bar{V}_j is an undetermined multiplier which cannot as yet be associated with its interpretation as a displacement component. An arbitrary variation of the rib strain energy can now be written

$$\Delta U_R + \Delta U_V = \sum_{j=1}^n \frac{4ab}{\mu \bar{t}} \bar{S}_j \delta \bar{S}_j + \sum_{j=1}^n 4a \bar{V}_j \left\{ \frac{1}{2a} \int_{-a}^a (\delta S_{j+1} - \delta S_j) d\mathbf{y} - \delta \bar{S}_j \right\}.$$

This completes the formulation of the total strain energy stored in the structure but it does remain to impose the further restraints on the arbitrary variations such that the state of overall equilibrium is undisturbed. From equations (34) and (35) these restraints are

$$U_E = \sum_{j=1}^n 2b \bar{w}_{0j} \left\{ S_{Rj+1} - S_{Rj} + S_{Fj+1} - S_{Fj} - \frac{W_j}{2b} \right\} \\ + \sum_{j=1}^n b (\bar{w}_{Rj} - \bar{w}_{Fj}) \left\{ S_{Rj+1} - S_{Rj} - S_{Fj+1} + S_{Fj} - 2\bar{S}_j - \frac{M_j}{4ab} \right\}$$

where \bar{w}_{0j} and $(\bar{w}_{Rj} - \bar{w}_{Fj})$ are undetermined multipliers which as cannot yet be associated with their interpretations as deflections. In this last expression it has been found convenient to make a substitution from equation (36). Subjecting this to an arbitrary variation

$$\Delta U_E = \sum_{j=1}^n 2b \bar{w}_{0j} \{ \delta S_{Rj+1} - \delta S_{Rj} + \delta S_{Fj+1} - \delta S_{Fj} \} \\ + \sum_{j=1}^n b (\bar{w}_{Rj} - \bar{w}_{Fj}) \{ \delta S_{Rj+1} - \delta S_{Rj} - \delta S_{Fj+1} + \delta S_{Fj} - 2\delta \bar{S}_j \}.$$

The total strain energy stored in the swept wing structure is thus

$$U = U_S + U_B + U_W + U_R$$

and it is seen that an arbitrary variation is

$$\Delta U = \Delta U_S + \Delta U_U + \Delta U_B + \Delta U_{U_{R,F}} + \Delta U_W + \Delta U_R + \Delta U_V + \Delta U_E$$

which must be zero for the strain energy to be a minimum.

By the usual arguments of the Calculus of Variations it will be found for the vanishing of the variation $\int_{-a}^a \delta S_j d\mathbf{y}$ it is necessary that

$$\frac{L}{\mu \bar{t}} S_j \sin \alpha + \frac{1}{Et^*} \left\{ -\frac{L^3}{3} \frac{d^2 S_j}{d\mathbf{y}^2} \operatorname{cosec} \alpha + \frac{L^2}{2} \frac{d\bar{T}_{j-1}}{d\mathbf{y}} \operatorname{cosec} \alpha \right. \\ \left. + 4LS_j \cot \alpha \cos \alpha + 2L\bar{T}_{j-1} \cot \alpha \right\} - L \frac{d\bar{U}_j}{d\mathbf{y}} = \bar{V}_j - \bar{V}_{j-1}$$

and for the variation $\int_{-a}^a \delta \bar{T}_{j-1} d\mathbf{y}$ it is necessary that

$$\bar{U}_j = \frac{1}{Et^*} \left\{ -\frac{L^2}{2} \frac{dS_j}{d\mathbf{y}} \operatorname{cosec} \alpha + L\bar{T}_{j-1} \operatorname{cosec} \alpha + 2LS_j \cot \alpha \right\} + \bar{U}_{j-1}.$$

These are consistent with equations (10) and (12) and it will be noted that the undetermined multipliers are in fact the displacement components \bar{U}_j and \bar{V}_j .

Proceeding in like manner, it is found for the vanishing of the variations $\delta\bar{P}_{Rj-1}$ and $\delta\bar{P}_{Fj-1}$ it is respectively necessary that

$$\bar{\mathbf{U}}_{Rj} = \frac{1}{EA_R} \left[\frac{L^2}{2} \{S_{Rj} + S_j(a)\} + L\bar{P}_{Rj-1} \right] + \bar{\mathbf{U}}_{Rj-1}$$

and

$$\bar{\mathbf{U}}_{Fj} = \frac{1}{EA_F} \left[\frac{L^2}{2} \{S_{Fj} - S_j(-a)\} + L\bar{P}_{Fj-1} \right] + \bar{\mathbf{U}}_{Fj-1}.$$

These are identical with equations (22) and (26) and it will be noted that the undetermined multipliers are in fact the displacement components $\bar{\mathbf{U}}_{Rj}$ and $\bar{\mathbf{U}}_{Fj}$.

The vanishing of the variations $\delta S_j(a)$ and $\delta S_j(-a)$ respectively requires that

$$\begin{aligned} & \left[\frac{1}{Et^*} \left\{ \frac{L^3}{3} \frac{dS_j}{dy} \operatorname{cosec} \alpha - \frac{L^2}{2} \bar{\mathbf{T}}_{j-1} \operatorname{cosec} \alpha - L^2 S_j \cot \alpha \right\} + L\bar{\mathbf{U}}_j \right]_{y=a} \\ & = -\frac{1}{EA_R} \left[\frac{L^3}{3} \{S_{Rj} + S_j(a)\} + \frac{L^2}{2} \bar{P}_{Rj-1} \right] + L\bar{\mathbf{U}}_{Rj} \end{aligned}$$

and

$$\begin{aligned} & \left[\frac{1}{Et^*} \left\{ \frac{L^3}{3} \frac{dS_j}{dy} \operatorname{cosec} \alpha - \frac{L^2}{2} \bar{\mathbf{T}}_{j-1} \operatorname{cosec} \alpha - L^2 S_j \cot \alpha \right\} + L\bar{\mathbf{U}}_j \right]_{y=-a} \\ & = -\frac{1}{EA_F} \left[\frac{L^3}{3} \{S_{Fj} - S_j(-a)\} + \frac{L^2}{2} \bar{P}_{Fj-1} \right] + L\bar{\mathbf{U}}_{Fj}. \end{aligned}$$

It will be found that these last two are respectively identical with equations (21) and (25) when substitutions are made from equations (23), (24), (27) and (28).

The vanishing of the variation $\delta\bar{S}_j$ requires that

$$(\bar{w}_{Rj} - \bar{w}_{Fj}) = \frac{2a}{\mu\bar{t}} \bar{S}_j - \frac{2a}{b} \bar{V}_j$$

which corresponds to equation (29) and where it is seen that once again the undetermined multiplier corresponds with the displacement difference $\bar{w}_{Rj} - \bar{w}_{Fj}$.

Finally, the vanishing of the variations δS_{Rj} and δS_{Fj} respectively requires that

$$\begin{aligned} & \frac{1}{EA_R} \left[\frac{L^3}{3} \{S_{Rj} + S_j(a)\} + \frac{L^2}{2} \bar{P}_{Rj-1} \right] - L\bar{\mathbf{U}}_{Rj} + \frac{Lb}{\mu\bar{t}_R} S_{Rj} + b(\bar{w}_{0j-1} - \bar{w}_{0j}) \\ & + \frac{b}{2} (\bar{w}_{Rj-1} - \bar{w}_{Fj-1} - \bar{w}_{Rj} + \bar{w}_{Fj}) = 0 \end{aligned}$$

and

$$\begin{aligned} & \frac{1}{EA_F} \left[\frac{L^3}{3} \{S_{Fj} - S_j(-a)\} + \frac{L^2}{2} \bar{P}_{Fj-1} \right] - L\bar{\mathbf{U}}_{Fj} + \frac{Lb}{\mu\bar{t}_F} S_{Fj} + b(\bar{w}_{0j-1} - \bar{w}_{0j}) \\ & - \frac{b}{2} (\bar{w}_{Rj-1} - \bar{w}_{Fj-1} + \bar{w}_{Rj} - \bar{w}_{Fj}) = 0. \end{aligned}$$

It will be found on substitution from equations (23), (27) and (29) that these last two equations correspond with equations (32) and (33). The undetermined multiplier of course corresponds with the displacement \bar{w}_{0j} .

It has therefore been demonstrated that the foregoing procedure is consistent with the total strain energy stored in the structure being rendered a minimum.

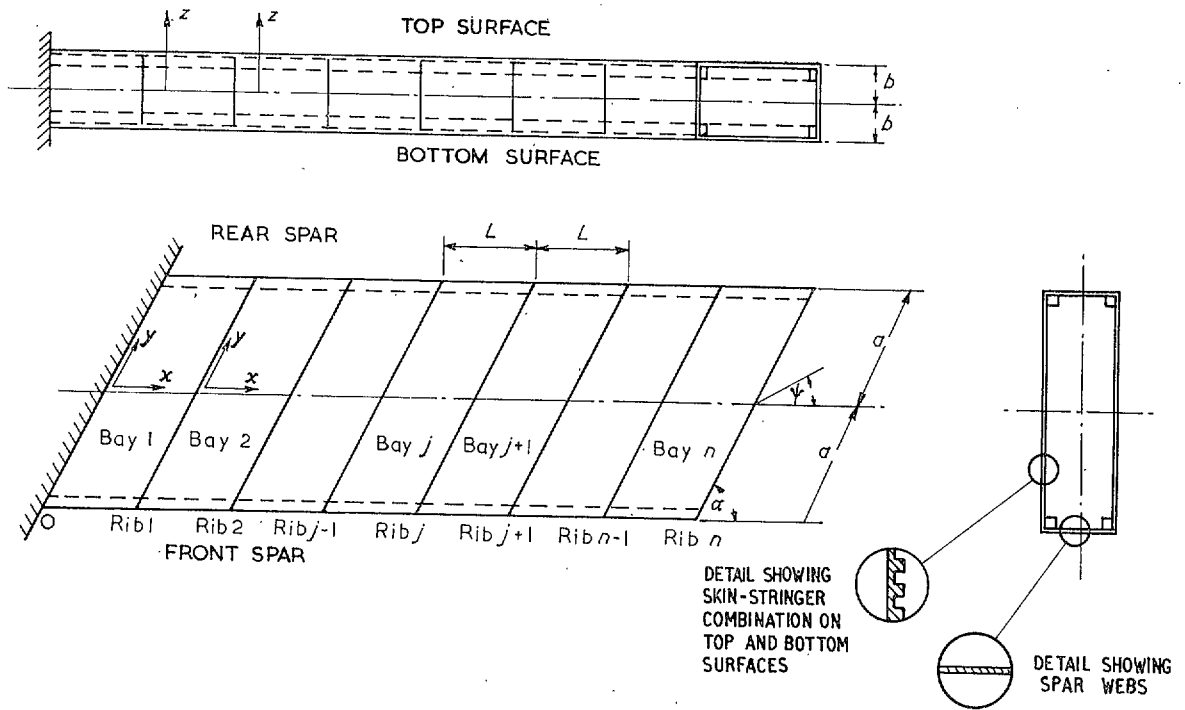


FIG. 1. The cantilever swept-back wing structure.

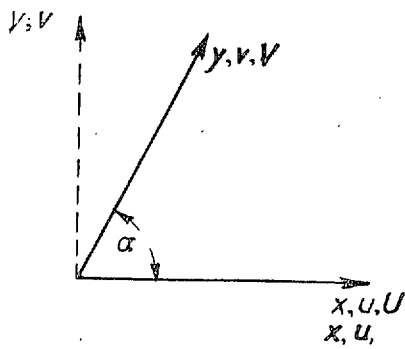


FIG. 2. Oblique and rectangular co-ordinate systems

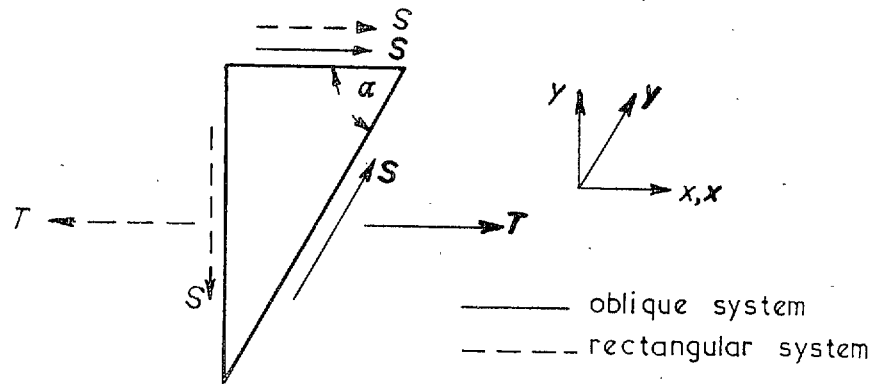


FIG. 3. Oblique and rectangular systems of stress resultants.

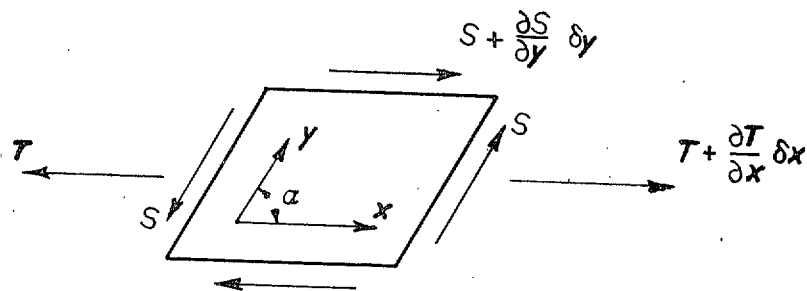


FIG. 4. Oblique system of stress resultants acting on an elemental portion of the skin-stringer combination.

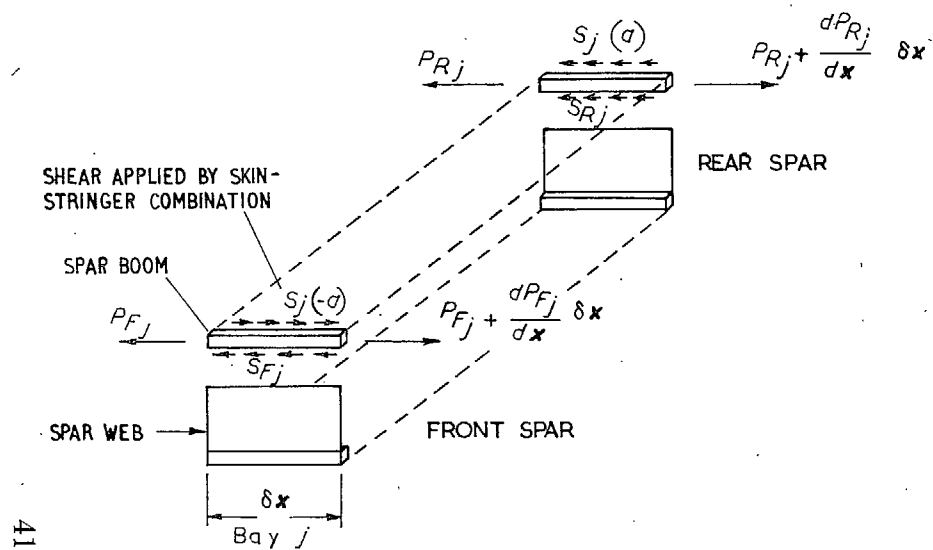


FIG. 5. Forces acting on elemental portions of the spar booms in the j th bay

41

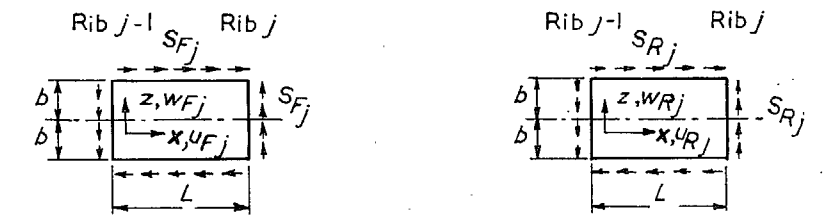


FIG. 7. Co-ordinate systems for and forces acting on the front and rear spar webs in the j th bay.

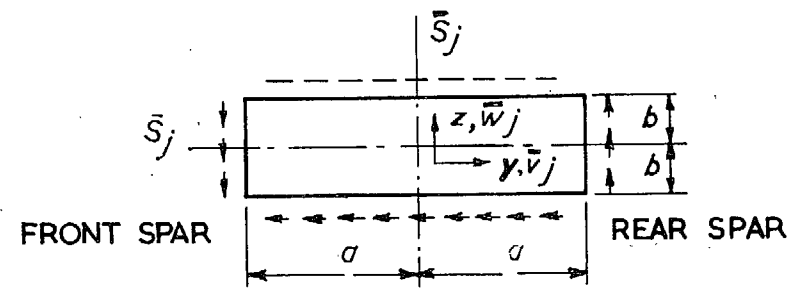
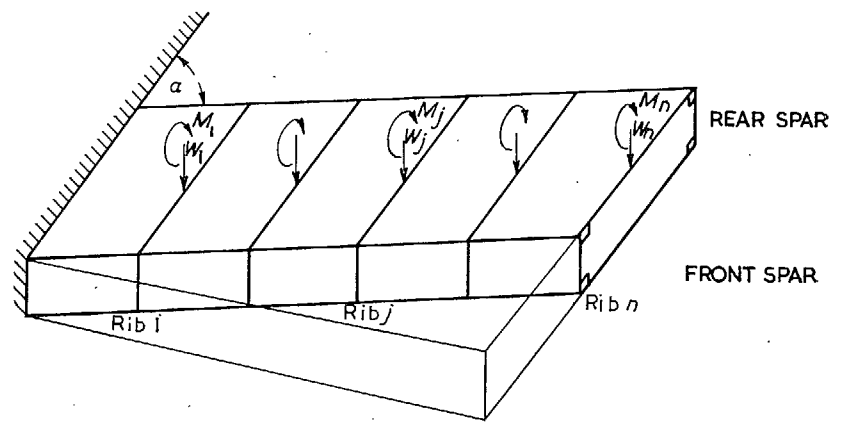


FIG. 6. Co-ordinate system for and forces acting on the j th rib.

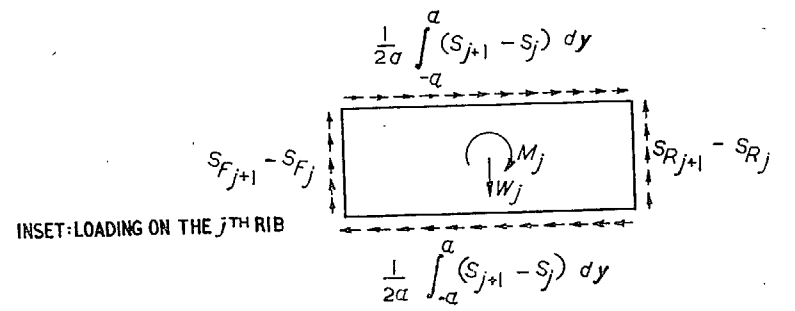


FIG. 8. System of loading applied to swept-back wing structure with inset showing loading on the j th rib.

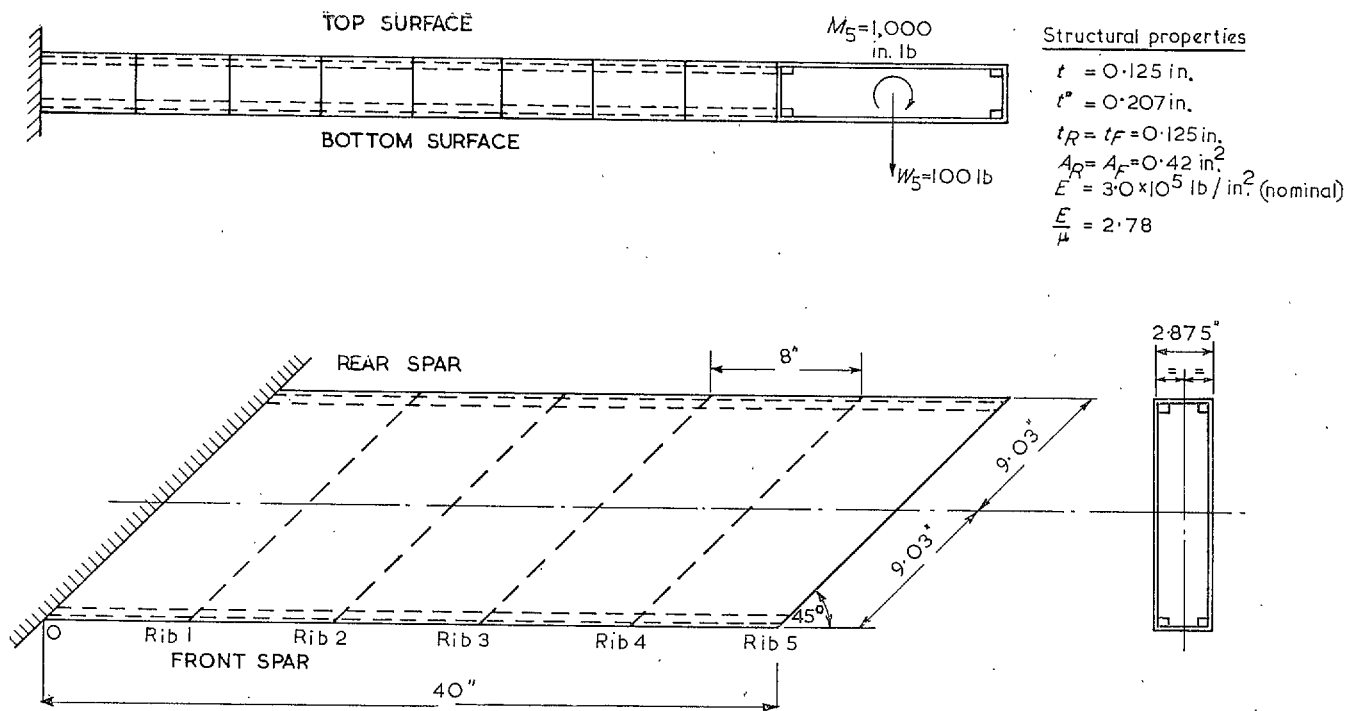


FIG. 9. Details of swept-back wing used for numerical calculations.

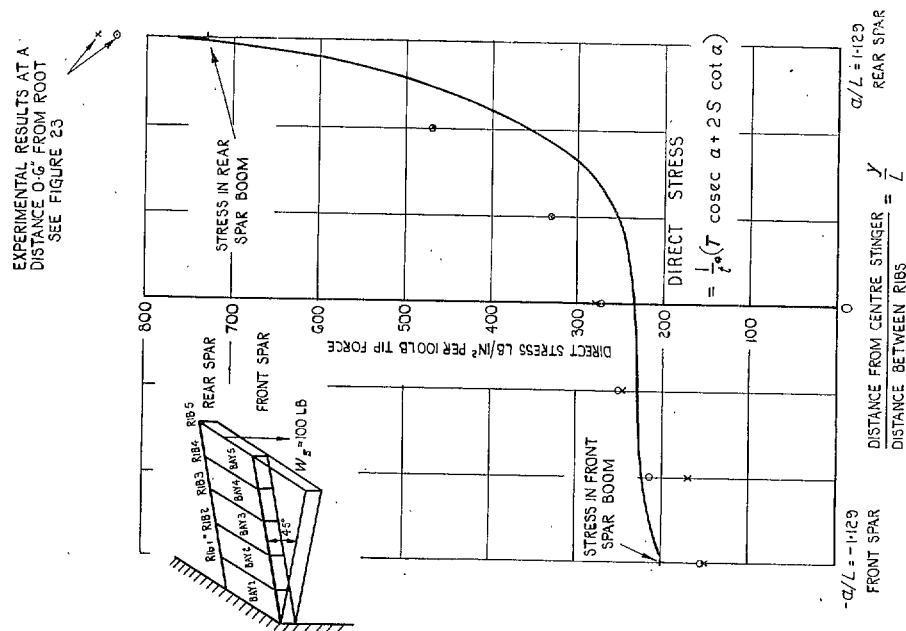


FIG. 10. Direct stress along the stringers plotted along the root section (*i.e.*, Rib 0) for tip force normal to the plane of the wing.

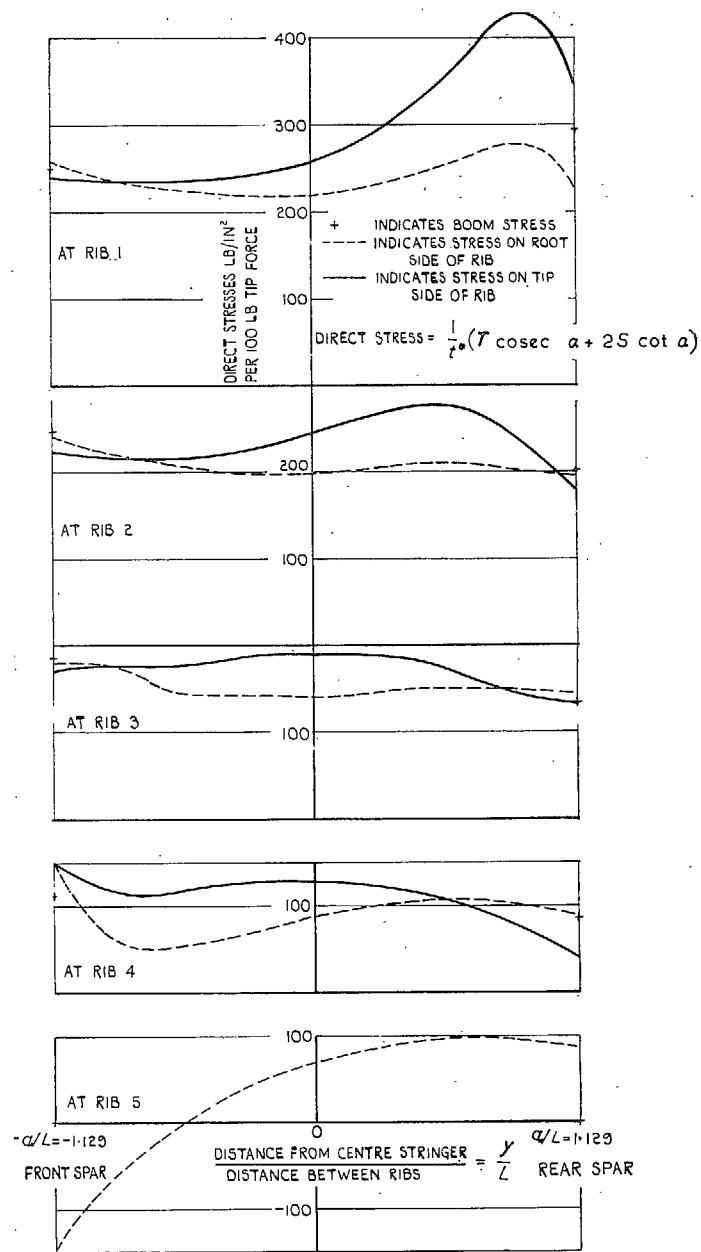


FIG. 11. Direct stress along the stringers plotted along ribs 1 to 5 for tip force normal to the plane of the wing.

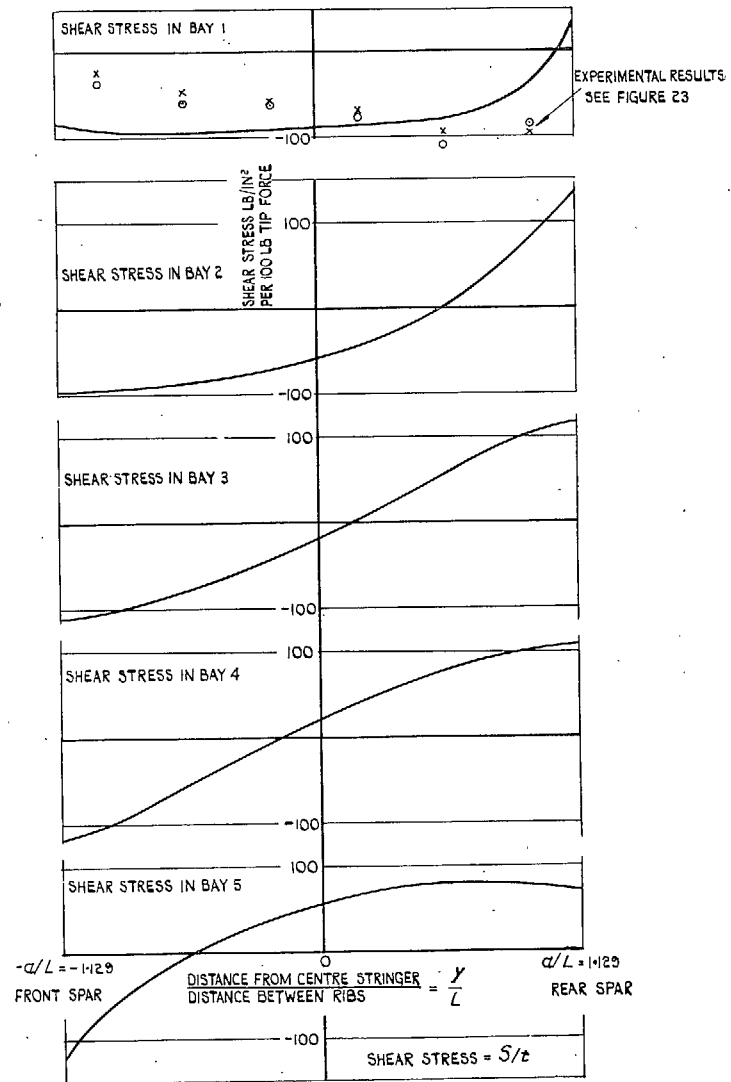


FIG. 12. Shear stresses in the skin-stringer combination for tip force normal to the plane of the wing.

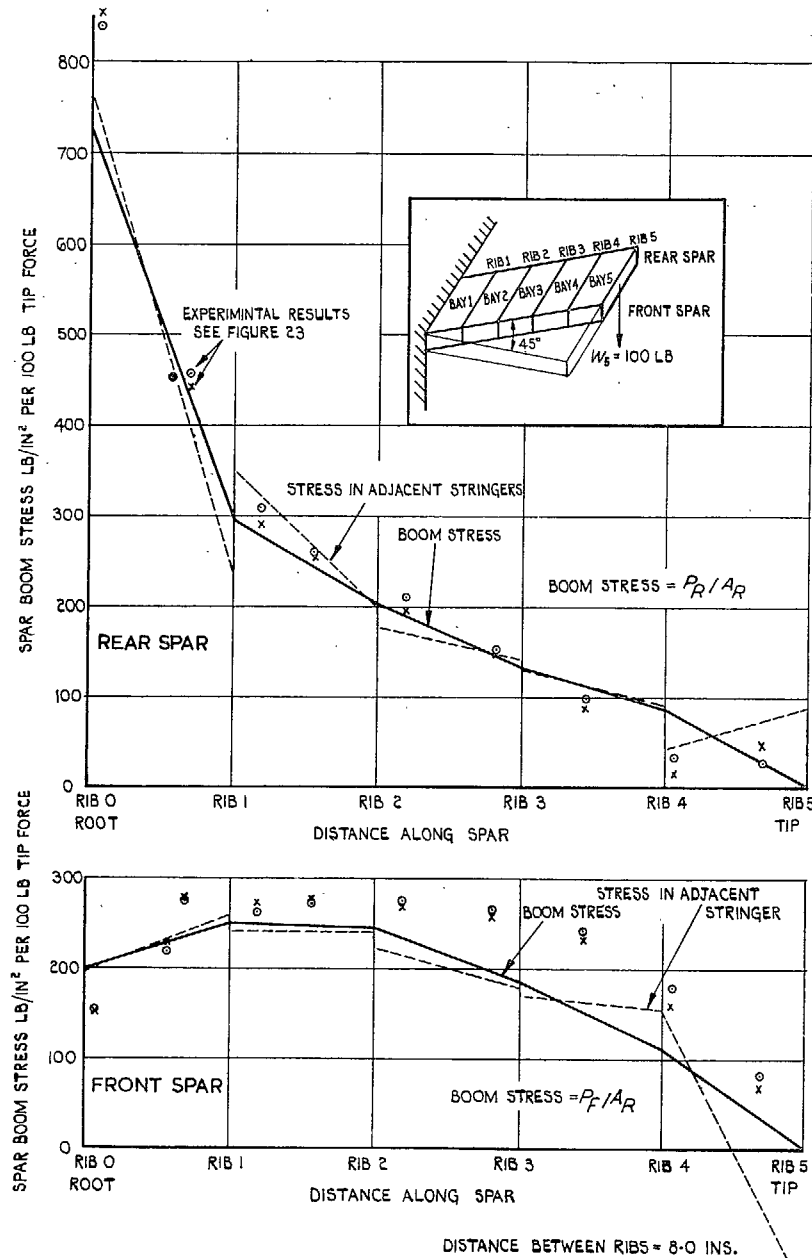


FIG. 13. Spanwise distribution of front and rear spar boom stresses for tip force normal to the plane of the wing.

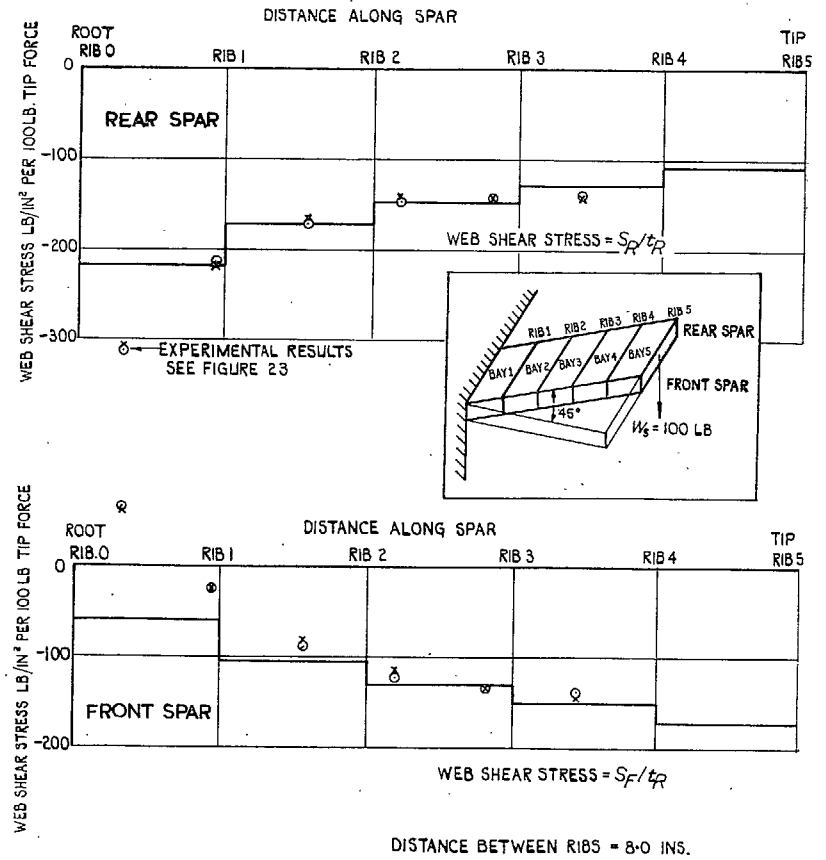


FIG. 14. Spanwise distribution of web shear stresses in the front and rear spars for tip force normal to the plane of the wing.

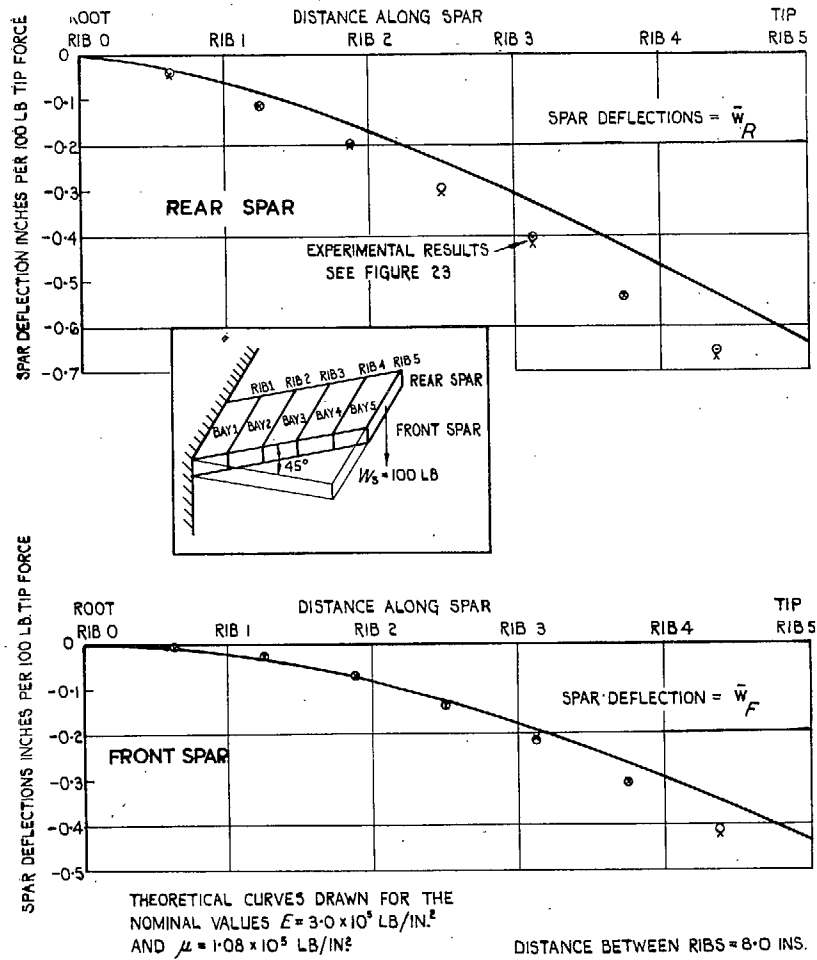


FIG. 15. Front and rear spar deflections for tip force normal to the plane of the wing.

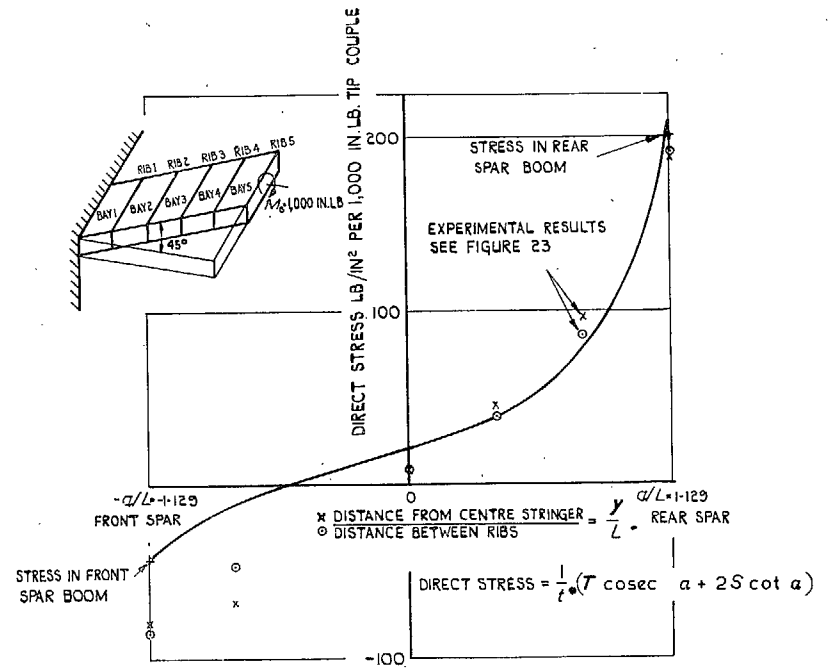


FIG. 16. Direct stress along the stringer plotted along the root section (i.e., rib 0) for tip couple in the plane of the rib.

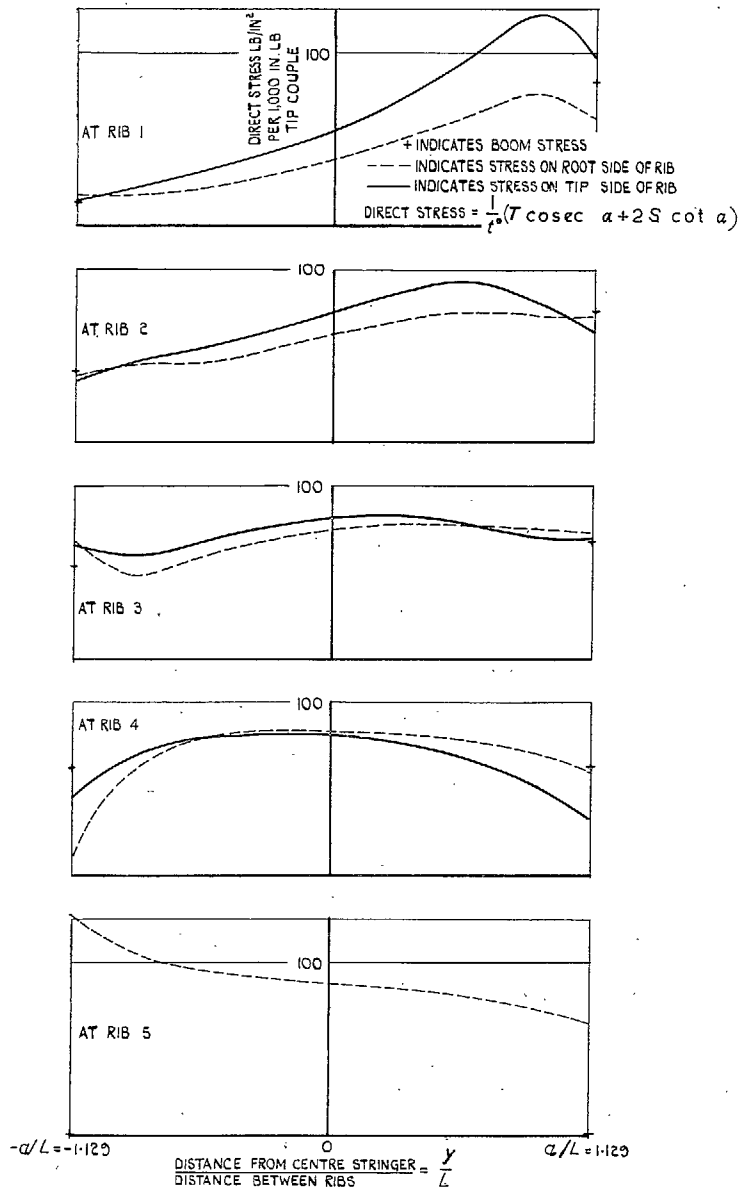


FIG. 17. Direct stress along the stringers plotted along ribs 1 to 5 for tip couple in the plane of the rib.

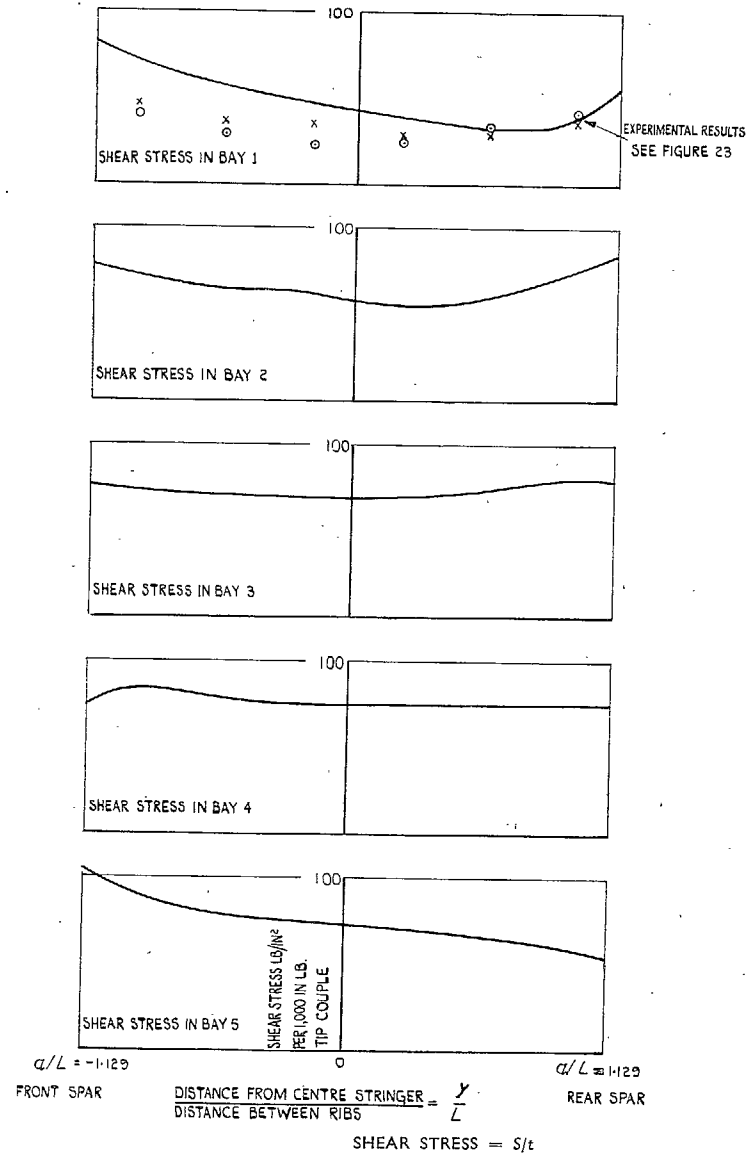


FIG. 18. Shear stresses in the skin-stringer combination for tip couple in the plane of the rib.

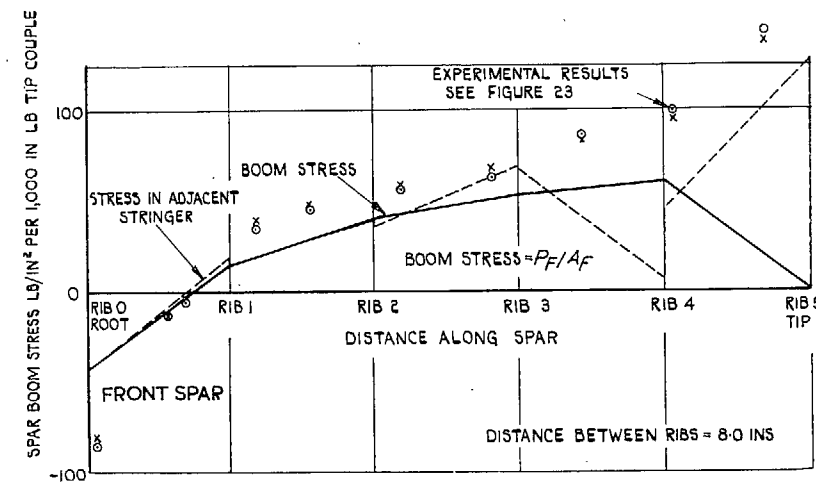
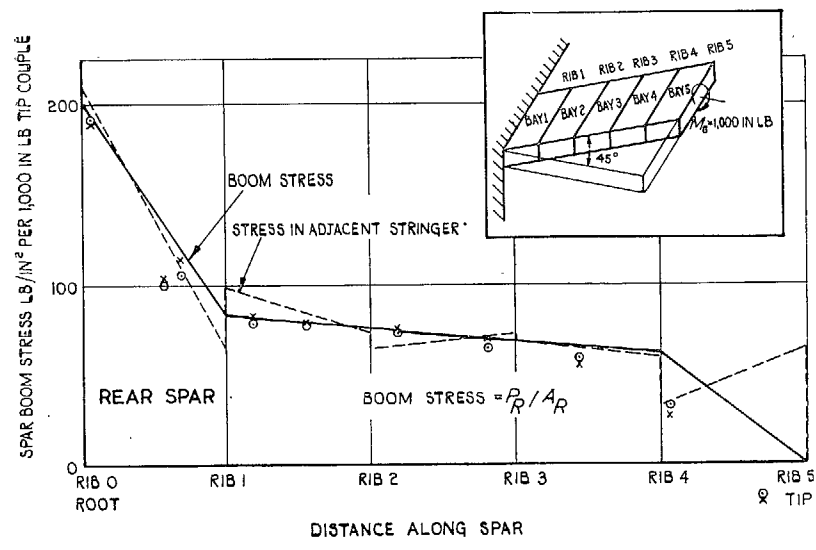


FIG. 19. Spanwise distribution of front and rear spar boom stresses for tip couple in the plane of the rib.

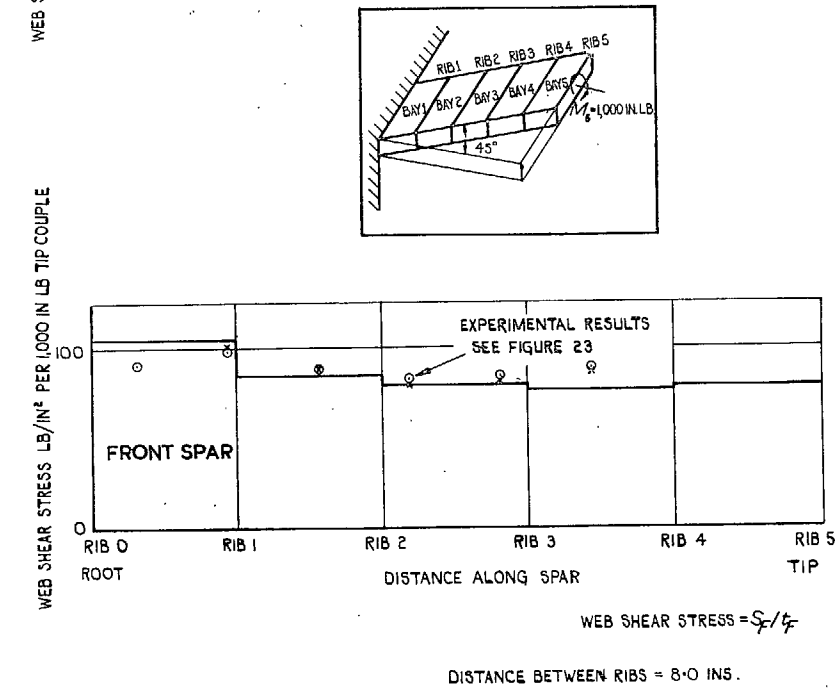
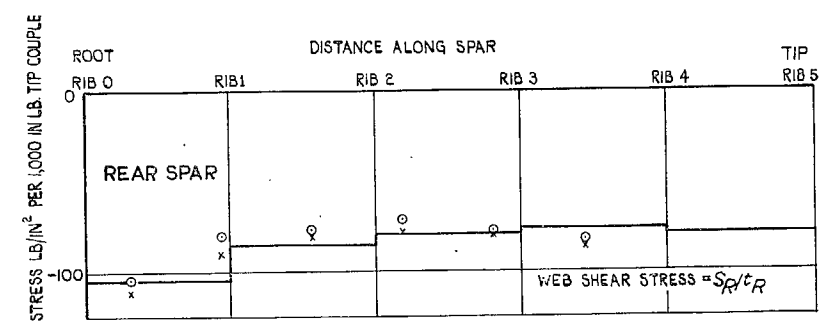
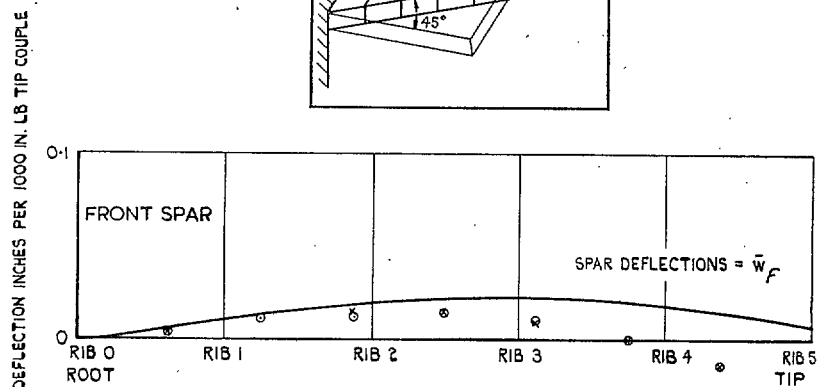
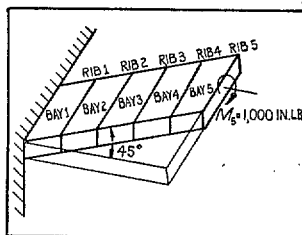
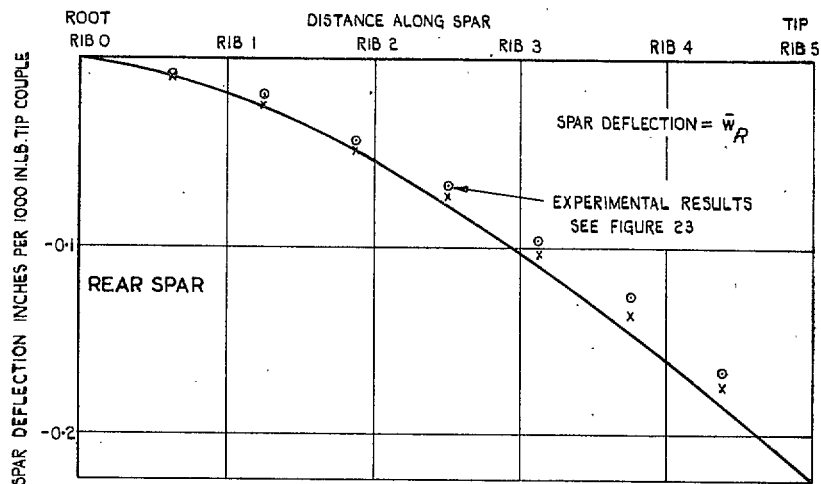


FIG. 20. Spanwise distribution of web shear stresses in front and rear spars for tip couple in the plane of the rib.



THEORETICAL CURVES DRAWN FOR THE
 NOMINAL VALUES $E = 3.0 \times 10^5$ LB/IN²
 AND $\mu = 1.08 \times 10^5$ LB/IN²

DISTANCE BETWEEN RIBS = 8.0 INS

FIG. 21. Front and rear spar deflections for tip couple in the plane of the rib.

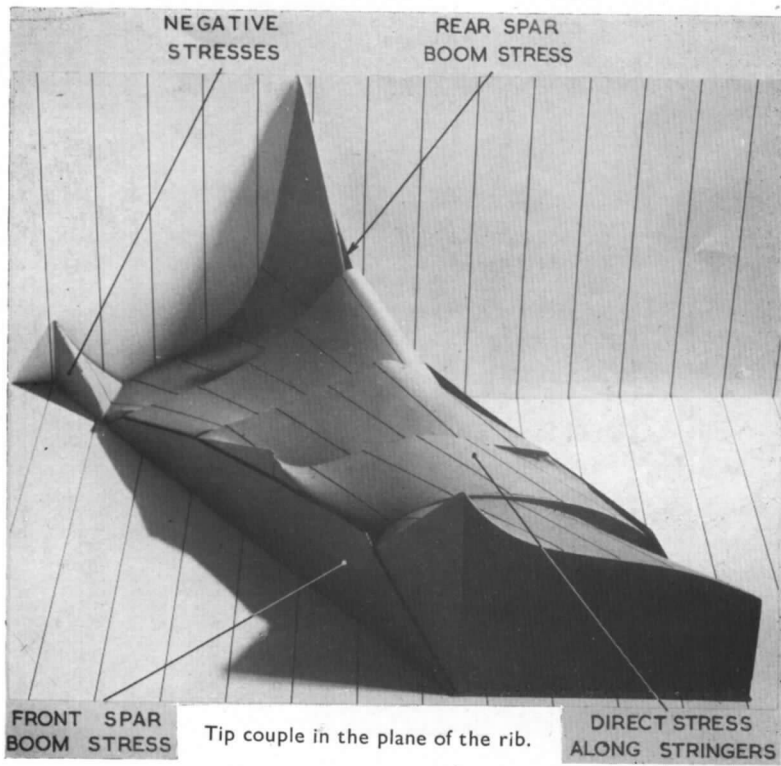
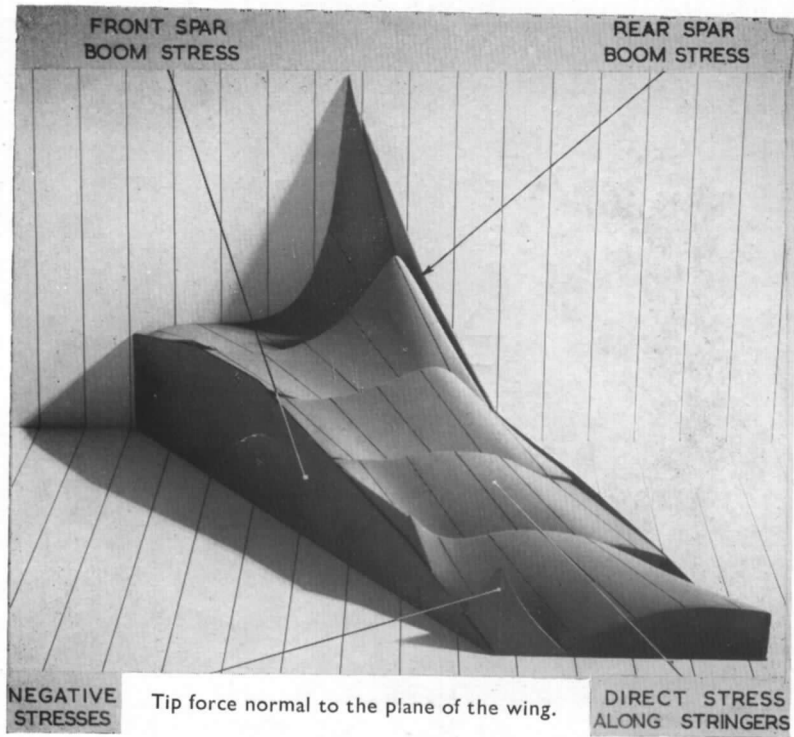


FIG. 22. Panoramic views of the direct stresses along the stringers and spar booms for tip force normal to the plane of the wing, and tip couple in the plane of the rib.

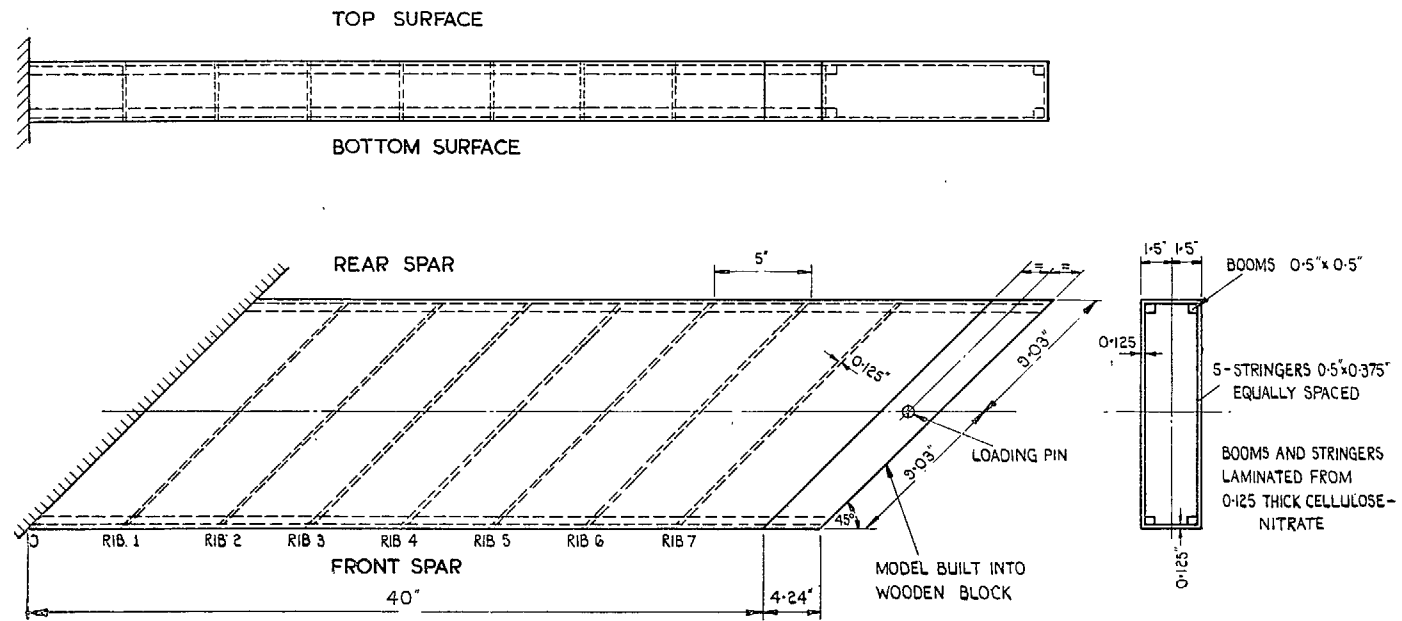


FIG. 23. Details of cellulose-nitrate model swept-back wing used for experiment.

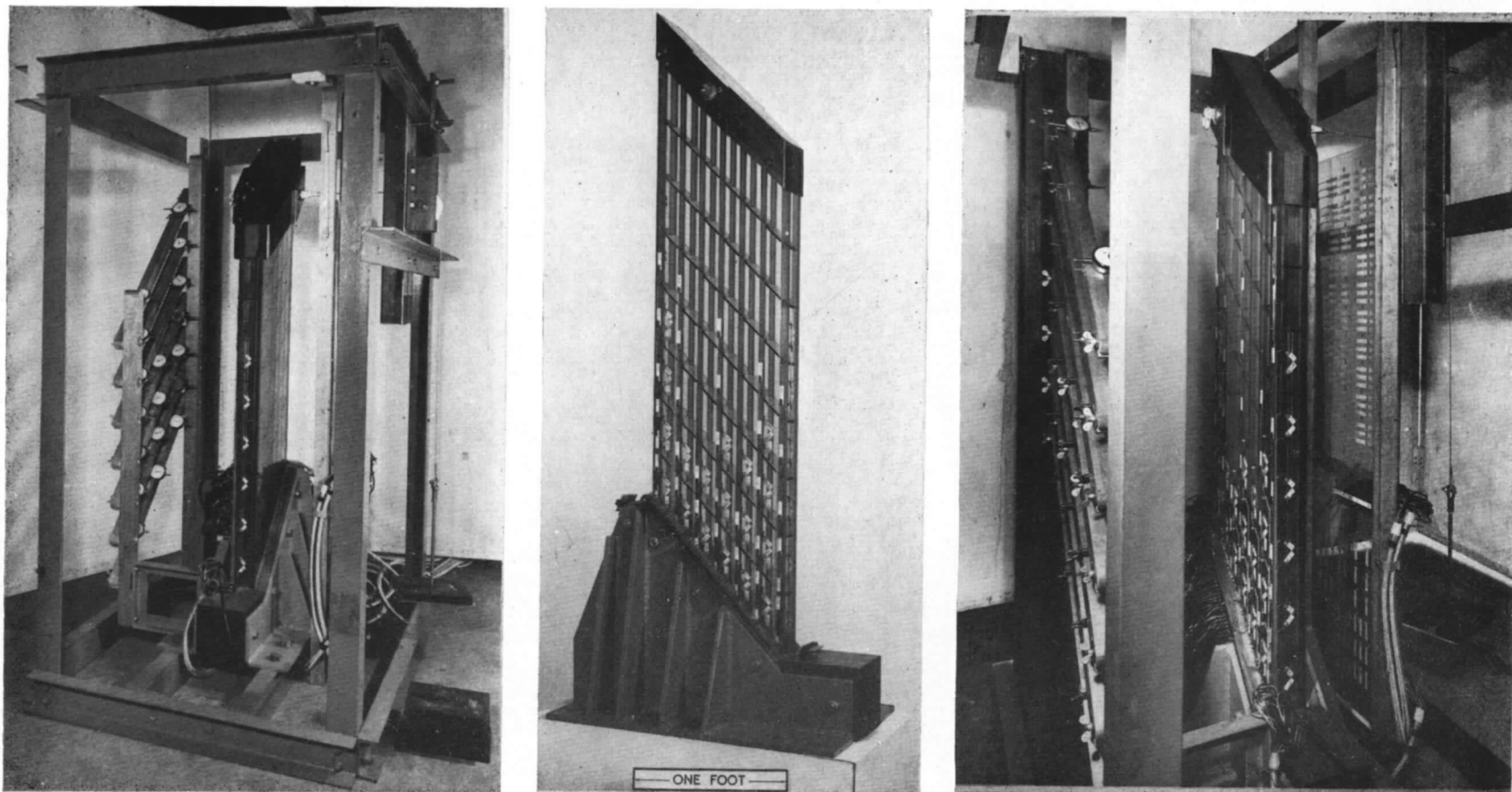


FIG. 24. Cellulose-nitrate model and test rig.

Publications of the Aeronautical Research Council

ANNUAL TECHNICAL REPORTS OF THE AERONAUTICAL RESEARCH COUNCIL (BOUND VOLUMES)

- 1939 Vol. I. Aerodynamics General, Performance, Airscrews, Engines. 50s. (51s. 9d.)
Vol. II. Stability and Control, Flutter and Vibration, Instruments, Structures, Seaplanes, etc. 63s. (64s. 9d.)
- 1940 Aero and Hydrodynamics, Aerofoils, Airscrews, Engines, Flutter, Icing, Stability and Control, Structures, and a miscellaneous section. 50s. (51s. 9d.)
- 1941 Aero and Hydrodynamics, Aerofoils, Airscrews, Engines, Flutter, Stability and Control, Structures. 63s. (64s. 9d.)
- 1942 Vol. I. Aero and Hydrodynamics, Aerofoils, Airscrews, Engines. 75s. (76s. 9d.)
Vol. II. Noise, Parachutes, Stability and Control, Structures, Vibration, Wind Tunnels. 47s. 6d. (49s. 3d.)
- 1943 Vol. I. Aerodynamics, Aerofoils, Airscrews. 80s. (81s. 9d.)
Vol. II. Engines, Flutter, Materials, Parachutes, Performance, Stability and Control, Structures. 90s. (92s. 6d.)
- 1944 Vol. I. Aero and Hydrodynamics, Aerofoils, Aircraft, Airscrews, Controls. 84s. (86s. 3d.)
Vol. II. Flutter and Vibration, Materials, Miscellaneous, Navigation, Parachutes, Performance, Plates and Panels, Stability, Structures, Test Equipment, Wind Tunnels. 84s. (86s. 3d.)
- 1945 Vol. I. Aero and Hydrodynamics, Aerofoils. 130s. (132s. 6d.)
Vol. II. Aircraft, Airscrews, Controls. 130s. (132s. 6d.)
Vol. III. Flutter and Vibration, Instruments, Miscellaneous, Parachutes, Plates and Panels, Propulsion. 130s. (132s. 3d.)
Vol. IV. Stability, Structures, Wind tunnels, Wind Tunnel Technique. 130s. (132s. 3d.)

ANNUAL REPORTS OF THE AERONAUTICAL RESEARCH COUNCIL—

1937 2s. (2s. 2d.) 1938 1s. 6d. (1s. 8d.) 1939-48 3s. (3s. 3d.)

INDEX TO ALL REPORTS AND MEMORANDA PUBLISHED IN THE ANNUAL TECHNICAL REPORTS, AND SEPARATELY—

April, 1950 - - - - - R. & M. No. 2600. 2s. 6d. (2s. 8d.)

AUTHOR INDEX TO ALL REPORTS AND MEMORANDA OF THE AERONAUTICAL RESEARCH COUNCIL—

1909-January, 1954 - - - - - R. & M. No. 2570. 15s. (15s. 6d.)

INDEXES TO THE TECHNICAL REPORTS OF THE AERONAUTICAL RESEARCH COUNCIL—

December 1, 1936 — June 30, 1939. R. & M. No. 1850. 1s. 3d. (1s. 5d.)
July 1, 1939 — June 30, 1945. - R. & M. No. 1950. 1s. (1s. 2d.)
July 1, 1945 — June 30, 1946. - R. & M. No. 2050. 1s. (1s. 2d.)
July 1, 1946 — December 31, 1946. R. & M. No. 2150. 1s. 3d. (1s. 5d.)
January 1, 1947 — June 30, 1947. - R. & M. No. 2250. 1s. 3d. (1s. 5d.)

PUBLISHED REPORTS AND MEMORANDA OF THE AERONAUTICAL RESEARCH COUNCIL—

Between Nos. 2251-2349. - - R. & M. No. 2350. 1s. 9d. (1s. 11d.)
Between Nos. 2351-2449. - - R. & M. No. 2450. 2s. (2s. 2d.)
Between Nos. 2451-2549. - - R. & M. No. 2550. 2s. 6d. (2s. 8d.)
Between Nos. 2551-2649. - - R. & M. No. 2650. 2s. 6d. (2s. 8d.)

Prices in brackets include postage

HER MAJESTY'S STATIONERY OFFICE

York House, Kingsway, London W.C.2; 423 Oxford Street, London W.1;
13a Castle Street, Edinburgh 2; 39 King Street, Manchester 2; 2 Edmund Street, Birmingham 3; 109 St. Mary Street,
Cardiff; Tower Lane, Bristol 1; 80 Chichester Street, Belfast, or through any bookseller